Enforced η^1-Fluorenyl and Indenyl Coordination to Zirconium: Geometrically Constrained and Sterically Expanded Complexes Derived from the Bifunctional $(FluPPh_2NAr)^-$ and $(IndPPh_2NAr)^-$ Ligands

Pascal Oulié,[†] Christelle Freund,[†] Nathalie Saffon,[‡] Blanca Martin-Vaca,*[,†] Laurent Maron,*[,§] and Didier Bourissou*[,†]

Laboratoire Hétérochimie Fondamentale et Appliquée du CNRS (UMR 5069), Université Paul Sabatier, 118, route de Narbonne, F-31062 Toulouse Cedex 09, France, Structure Fédérative Toulousaine en Chimie Moléculaire (FR 2599) Université Paul Sabatier, 118, route de Narbonne, F-31062 Toulouse Cedex 09, France, and Laboratoire de Physique et Chimie des Nanoobjets (UMR 5215), INSA, Université Paul Sabatier, 135, avenue de Rangueil, F-31077 Toulouse Cedex, France

Received October 1, 2007

The $(FluPPh_2NAr)$ and $(IndPPh_2NAr)$ ligands **2a–c** and **4a–c** (**a**, Ar = Ph; **b**, R = DIPP; **c**, = Mes) were readily prepared by Staudinger reactions between aryl azides and Flu/Ind diphenylphosphines, and they were coordinated to zirconium via toluene elimination. The propensity of the pendent phosphazene group to enforce low hapticity of the Flu and Ind rings in the ensuing complexes has been demonstrated experimentally and theoretically. Of particular interest, geometrically constrained and sterically expanded structures have been evidenced spectroscopically and structurally for both complexes $[(FluPPh_2NPh)ZrBn_3]$ **5a** and $[(IndPPh_2NPh)ZrBn_3]$ **7a**. In addition, the ability of the aryl substituent at nitrogen to modulate the hapticity of the Ind ring (from η^1, to η^2, and η^3) has been substantiated, and intramolecular CH-activation reactions leading to doubly cyclometalated complexes **6c** and **8c** have been observed when R = Mes.

Introduction

Cyclopentadienyl rings (Cp) and the related indenyl (Ind) and fluorenyl (Flu) systems are among the most commonly used ligands, with examples of their complexes across the periodic table. In particular, they have found enormous use in the preparation of Ziegler–Natta-type initiators for olefin polymerization.[1] Variation of the Cp substitution pattern has been extensively studied in order to tune the stereoelectronic properties around the metal, to control the orientation and rotation of the Cp-type ring (such as in ansa-metallocenes[2]), and to introduce functional groups that may interact with the metal center.[3,4] Constrained geometry complexes (CGCs) **A** (Figure 1) obtained by introduction of a short silylamido sidearm on a Cp-type ring clearly represent one of the most spectacular achievements in this area.[5]

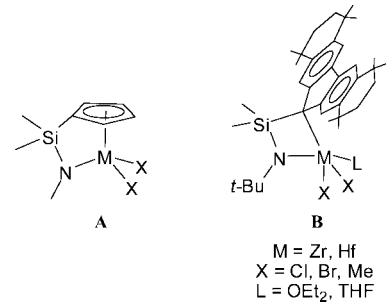

Figure 1. Structure of the archetypal CGCs **A** and of the geometrically constrained and sterically expanded Flu complexes **B**.

The modularity of the Ind and Flu ligands is further increased by their ability to accommodate several easily interconvertible

* To whom correspondence should be addressed. E-mail: dbouriss@chimie.ups-tlse.fr.
† Laboratoire Hétérochimie Fondamentale et Appliquée du CNRS.
‡ Structure Fédérative Toulousaine en Chimie Moléculaire.
§ Laboratoire de Physique et Chimie des Nanoobjets.

(1) (a) Brintzinger, H. H.; Fischer, D.; Mülhaupt, R.; Rieger, B.; Waymouth, R. M. *Angew. Chem., Int. Ed. Engl.* **1995**, *34*, 1143. (b) Bochmann, T. *J. Chem. Soc., Dalton Trans.* **1996**, 255. (c) Alt, H. G.; Köppl, A. *Chem. Rev.* **2000**, *100*, 1205. (d) Resconi, L.; Cavallo, L.; Fait, A.; Piemontesi, F. *Chem. Rev.* **2000**, *100*, 1253. (e) Lin, S.; Waymouth, R. M. *Acc. Chem. Res.* **2002**, *35*, 765.

(2) (a) Shapiro, P. J. *Coord. Chem. Rev.* **2002**, *231*, 67. (b) Prashar, S.; Antiñolo, A.; Otero, A. *Coord. Chem. Rev.* **2006**, *250*, 133. (c) Wang, B. *Coord. Chem. Rev.* **2006**, *250*, 242.

(3) Erker, G.; Kehr, G.; Fröhlich, R. *Coord. Chem. Rev.* **2006**, *250*, 36.

(4) For Cp metal complexes featuring pendant donor groups, see: (a) Jutzi, P.; Redeker, T. *Eur. J. Inorg. Chem.* **1998**, 663. (b) Siemeling, U. *Chem. Rev.* **2000**, *100*, 1495. (c) Butenschön, H. *Chem. Rev.* **2000**, *100*, 1527. (d) Piers, W. E. *Chem. Eur. J.* **1998**, *4*, 13. (e) Hill, M.; Erker, G.; Kehr, G.; Fröhlich, R.; Kataeva, O. *J. Am. Chem. Soc.* **2004**, *126*, 11046.

(5) (a) McKnight, A. L.; Waymouth, R. M. *Chem. Rev.* **1998**, *98*, 2587. (b) Gibson, V. C.; Spitmesser, S. K. *Chem. Rev.* **2003**, *103*, 283. (c) Braunschweig, H.; Breitling, F. M. *Coord. Chem. Rev.* **2006**, *250*, 2691–2720.

(6) (a) O'Connor, J. M.; Casey, C. P. *Chem. Rev.* **1987**, *87*, 307. (b) Calhorda, M. J.; Veiros, L. F. *Coord. Chem. Rev.* **1999**, *185–186*, 37. (c) Calhorda, M. J.; Veiros, L. F. *Comments Inorg. Chem.* **2001**, *22*, 375. (d) Calhorda, M. J.; Romão, C. C.; Veiros, L. F. *Chem. Eur. J.* **2002**, *8*, 868. (e) Zargarian, D. *Coord. Chem. Rev.* **2002**, *233–234*, 157.

(7) For zirconium sandwich complexes featuring η^9-indenyl ligands, see: (a) Bradley, C. A.; Keresztes, I.; Lobkovsky, E.; Young, V. G.; Chirik, P. J. *J. Am. Chem. Soc.* **2004**, *126*, 16937. (b) Veiros, L. F. *Chem. Eur. J.* **2005**, *11*, 2505. (c) Veiros, L. F. *Organometallics* **2006**, *25*, 2266. (d) Bradley, C. A.; Veiros, L. F.; Pun, D.; Lobkovsky, E.; Keresztes, I.; Chirik, P. J. J. *Am. Chem. Soc.* **2006**, *128*, 16600.

10.1021/om700974g CCC: $37.00 © 2007 American Chemical Society
Publication on Web 12/05/2007

hapticities (so-called "ring slippage").[6–8] In particular, low Ind and Flu hapticities, which increase accessibility for the incoming substrates for both geometric and electronic reasons, have attracted considerable interest.[9] Very significantly, Miller et al. recently reported for the η^1-complex **B**, featuring the sterically hindered $(FluSiMe_2N\text{-}t\text{-}Bu)^{2-}$ ligand (M = Zr, X = Cl, and L = Et_2O), an inverted preference for α-olefin over ethylene polymerization (with homopolymerization activity typically 6 times higher toward propylene versus ethylene at 25 °C) and unprecedented stereoselectivity (resulting in syndiotactic polypropylene with melting temperatures as high as 165 °C).[10a,b] This peculiar behavior further reinforces the interest for group 4 complexes featuring low coordinated Ind or Flu ligands, whose number and variety remain so far extremely limited. Indeed, the fluorenyl complexes **B**[10a,c] are the very unique examples of so-called geometrically constrained and sterically expanded[11] systems combining bent $C_{ipso}-Si-N$ bond angles (∼96°, in the typical range associated with CGCs **A**) and widened $Si-C_{ipso}\text{-}C_g$ bond angles (∼202°), resulting in *outward* pyramidalization of the C_{ipso} center (with the silicon atom and the metal being located on opposite sides of the Flu ring, in marked contrast with that observed with CGCs **A**). Only a few other η^1-complexes **C-H**[12–16] of group 4 metals (Figure 2) have been structurally characterized, the low Flu or Ind hapticity being typically favored by the presence of strongly donating coligands (η^5-Cp, η^5-Ind, η^5-Flu, alkoxy, phosphinimide).[17,18]

In this context, we recently initiated a research program aimed at exploring the coordination chemistry of bifunctional $(CpPR_2NR')^-$ ligands,[19] formally deriving from the well-known

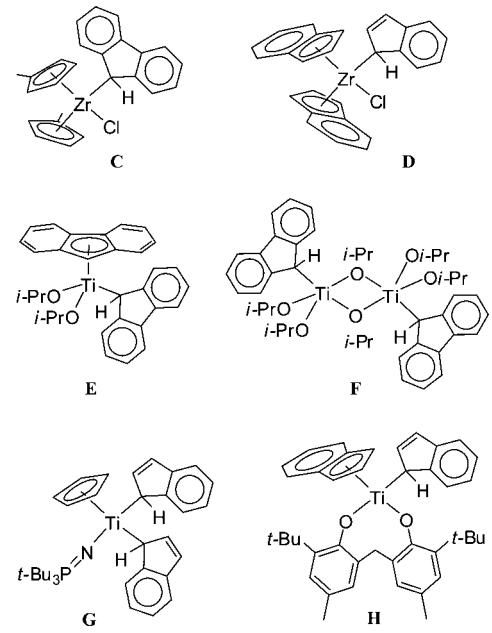

Figure 2. Structurally characterized η^1-fluorenyl and η^1-indenyl/group 4 metal complexes **C**−**H**.

1-aza-2-phospha(V)allyl ligands.[20–24] The presence of the short and strongly donating phosphazene sidearm[25] was expected to influence dramatically the bonding mode of the Cp-type ring,[26] as evidenced in the κ^2-N,C[(FluPPh$_2$NPh)Rh(nbd)] complex.[27] In addition, coordination to group 4 metals was expected to

(8) For η^4- and η^6-indenyl coordination through the benzo ring, see: (a) Bradley, C. A.; Lobkovsky, E.; Chirik, P. J. *J. Am. Chem. Soc.* **2003**, *125*, 8110. (b) Wang, S.; Tang, X.; Vega, A.; Saillard, J. -Y.; Sheng, E.; Yang, G.; Zhou, S.; Huang, Z *Organometallics* **2006**, *25*, 2399.

(9) For recent reviews on η^1-fluorenyl and η^1-indenyl complexes, see: (a) Alt, H. G.; Samuel, E. *Chem. Soc. Rev.* **1998**, *27*, 323. (b) Stradiotto, M.; McGlinchey, M. J. *Coord. Chem. Rev.* **2001**, *219–221*, 311. (c) Carpentier, J.-F.; Saillard, J.-Y.; Kirillov, E. *Coord. Chem. Rev.* **2005**, *249*, 1221.

(10) (a) Irwin, L. J.; Reibenspies, J. H.; Miller, S. A. *J. Am. Chem. Soc.* **2004**, *126*, 16716. (b) Irwin, L. J.; Miller, S. A. *J. Am. Chem. Soc.* **2005**, *127*, 9972. (c) Irwin, L. J.; Reibenspies, J. H.; Miller, S. A. *Polyhedron* **2005**, *24*, 1314. (d) Schwerdtfeger, E. D.; Miller, S. A. *Macromolecules* **2007**, *40*, 5662.

(11) The term "sterically-expanded", introduced for complexes featuring mono- and bis(tetramethylbenzo)fluorenyl substituents (Miller, S. A.; Bercaw, J. E. *Organomeyallics* **2004**, *23*, 1777), refers here to the open structure that is induced by the low hapticity of the Cp-type ring and that increases the accessibility of the metal center.

(12) Schmidt, M. A.; Alt, H. G.; Milius, W. *J. Organomet. Chem.* **1997**, *541*, 3.

(13) Schmidt, M. A.; Alt, H. G.; Milius, W. *J. Organomet. Chem.* **1997**, *544*, 139.

(14) Knjazhanski, S. Y.; Cadenas, G.; Garcia, M.; Pérez, C. M.; Nifant'ev, I. E.; Kashulin, I. A.; Ivchenko, P. V.; Lyssenko, K. A. *Organometallics* **2002**, *21*, 3094.

(15) Guérin, F.; Beddie, C. L.; Stephan, D. W.; Spence, R. E.; Wirz, R. v. H. *Organometallics* **2001**, *20*, 3466.

(16) Brintzinger, H. H.; Gritzo, H.; Wieser, U. CCDC-230739, 2004.

(17) The introduction of a sterically demanding phenoxide sidearm was reported to induce η^1-indenyl coordination toward $Ta(NMe_2)_3$: (a) Thorn, M. G.; Fanwick, P. E.; Chesnut, R. W.; Rothwell, I. P. *Chem. Commun.* **1999**, 2543. (b) Thorn, M. G.; Parker, J. R.; Fanwick, P. E.; Rothwell, I. P. *Organometallics* **2003**, *22*, 4658. But η^5-coordination was retained in the related $Ti(NMe_2)_2$ and $Zr(NMe_2)_2$ complexes. (c) Turner, L. E.; Thorn, M. G.; Fanwick, P. E.; Rothwell, I. P. *Organometallics* **2004**, *23*, 4658.

(18) η^1-Fluorenyl coordination has also been found in the geometrically-constrained dimeric yttrium complex $[(FluSiMe_2N\text{-}t\text{-}Bu)YH(THF)_2]_2$. Harder, S. *Organometallics* **2005**, *24*, 373.

(19) Related Cp-phosphazene zirconium and lutetium complexes were reported to adopt η^5-coordination with phosphazene → metal interaction. (a) Truflandier, L.; Marsden, C. J.; Freund, C.; Martin-Vaca, B.; Bourissou, D. *Eur. J. Inorg. Chem.* **2004**, 1939. (b) Rufanov, K. A.; Petrov, A. R.; Kotov, V. V.; Laquai, F.; Sundermeyer, J. *Eur. J. Inorg. Chem.* **2005**, 3805.

(20) (a) Izod, K. *Coord. Chem. Rev.* **2002**, *227*, 153. (b) Steiner, A.; Zacchini, S.; Richards, P. I. *Coord. Chem. Rev.* **2002**, *227*, 193.

(21) For Li complexes, see: López-Ortiz, F. *Curr. Org. Synth.* **2006**, *3*, 187 and references therein.

(22) For Zr and Ti complexes, see: (a) Sarsfield, M. J.; Thornton-Pett, M.; Bochmann, M. *J. Chem. Soc., Dalton Trans.* **1999**, 3329. (b) Sarsfield, M. J.; Said, M.; Thornton-Pett, M.; Gerrard, L. A.; Bochmann, M. *J. Chem. Soc., Dalton Trans.* **2001**, 822. (c) Said, M.; Thornton-Pett, M.; Bochmann, M. *J. Chem. Soc., Dalton Trans.* **2001**, 2844. (d) Said, M.; Thornton-Pett, M.; Hughes, D. L.; Bochmann, M. *Inorg. Chim. Acta* **2007**, *360*, 1354.

(23) For late metal complexes, see: (a) Imhoff, P.; Nefkens, S. C. A.; Elsevier, C. J.; Goubitz, K.; Stam, C. H. *Organometallics* **1991**, *10*, 1421. (b) Imhoff, P.; van Asselt, R.; Ernsting, J. M.; Vrieze, K.; Elsevier, C. J.; Smeets, W. J. J.; Spek, A. L.; Kentgens, A. P. M. *Organometallics* **1993**, *12*, 1523. (c) Avis, M. W.; Vrieze, K.; Kooijman, H.; Veldman, N.; Spek, A. L.; Elsevier, C. J. *Inorg. Chem.* **1995**, *34*, 4092. (d) Avis, M. W.; Vrieze, K.; Ernsting, J. M.; Elsevier, C. J.; Veldman, N.; Spek, A. L.; Katti, K. V.; Barnes, C. L. *Organometallics* **1996**, *15*, 2376. (e) Masuda, J. D.; Wei, P.; Stephan, D. W. *Dalton Trans.* **2003**, 3500. (f) Smurnyy Bibal, C.; Pink, M.; Caulton, K. G *J. Am. Chem. Soc.* **2005**, *127*, 8944. (g) Fang, M.; Jones, N. D.; Lukowski, R.; Tjathas, J.; Ferguson, M. J.; Cavell, R. G. *Angew. Chem., Int. Ed.* **2006**, *45*, 3097.

(24) For main group complexes, see: (a) Hitchcock, P. B.; Lappert, M. F.; Wang, Z.-X. *J. Organomet. Chem.* **2006**, *691*, 2748. (b) Leung, W. P.; Wong, K. W.; Wang, Z. X.; Mak, T. C. W. *Organometallics* **2006**, *25*, 2037. (c) Alhomaidan, O.; Hollink, E.; Stephan, D. W. *Organometallics* **2007**, *26*, 3041.

(25) For selected references, see: (a) Reetz, M. T.; Bohres, E.; Goddard, R. *Chem. Commun.* **1998**, 935. (b) Sauthier, M.; Forniés-Cámer, J.; Toupet, L.; Réau, R. *Organometallics* **2000**, *19*, 553. (c) Spencer, L. P.; Altwer, R.; Wie, P.; Gelmini, L.; Gauld, J.; Stephan, D. W. *Organometallics* **2003**, *22*, 3841. (d) Kocher, N.; Leusser, D.; Murso, A.; Stalke, D. *Chem. Eur. J.* **2004**, *10*, 3622. (e) Boubekeur, L.; Ricard, L.; Mézailles, N.; Le Floch, P. *Organometallics* **2005**, *24*, 1065. (f) Co, T. T; Shim, S. C.; Cho, C. S.; Kim, T.-J.; Kang, S. O.; Han, W.-S.; Ko, J.; Kim, C.-K. *Organometallics* **2005**, *24*, 4824.

(26) Introduction of a pendant phosphine sulfide has recently allowed for the first structural characterization of an η^1-indenyl rhodium complex. (a) Wechsler, D.; McDonald, R.; Ferguson, M. J.; Stradiotto, M. *Chem. Commun.* **2004**, 2446. (b) Wechsler, D.; Myers, A.; McDonald, R.; Ferguson, M. J.; Stradiotto, M. *Inorg. Chem.* **2006**, *45*, 4562.

(27) Freund, C.; Barros, N.; Gornitzka, H.; Martin-Vaca, B.; Maron, L.; Bourissou, D. *Organometallics* **2006**, *25*, 4927.

Scheme 1. Synthesis of the Fluorenyl Ligands 2a–c

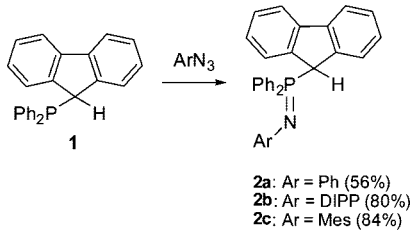

give access to a new type of phosphorus-containing analogues of CpSiN CGCs **A**.[28] We report here a detailed investigation of zirconium complexes deriving from $(FluPPh_2NAr)^-$ and $(IndPPh_2NAr)^-$, demonstrating that the pendent phosphazene can also enforce and modulate low hapticity of Flu and even Ind rings with group 4 metals. The geometrically constrained and sterically expanded structure of the resulting complexes is substantiated by X-ray analyses and DFT calculations. The substituent at nitrogen is shown to strongly influence the coordination mode, and CH-activation reactions leading to doubly cyclometalated complexes are reported.

Results and Discussion

Synthesis and Characterization of Ligands 2a–c and 4a–c. The fluorenyl ligands **2b** and **2c** featuring, respectively, the DIPP (2,6-diisopropylphenyl) and Mes (2,4,6-trimethylphenyl) susbtituent at the nitrogen atom were prepared following the same strategy than that previously reported for their phenylated analogue **2a**,[27] that is the Staudinger reaction between fluorenyldiphenylphosphine[29] and the corresponding aryl azides[30] (Scheme 1). As for **2a**, derivatives **2b** and **2c** adopt the tautomeric phosphazene form (N═P−CH) rather than the ylidic one (NH−P═C)[31] both in solution and in the solid state, as deduced from ^{13}C NMR spectroscopy (for both compounds, CH signals at ∼53 ppm were observed for the central C1 atom of the fluorenyl ring)[32] and from an X-ray diffraction analysis carried out for **2c** (the hydrogen atom at C1 could be located and refined without any constraint).[33]

Scheme 2. Synthesis of the Indenyl Ligands 4a–c

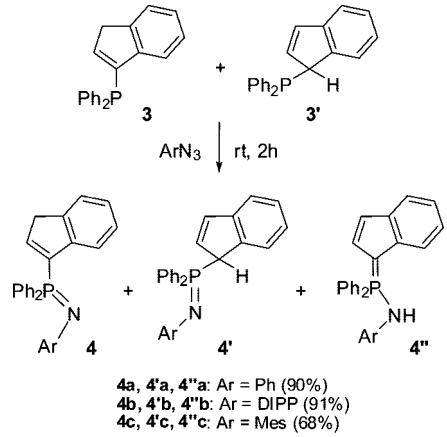

Following the same strategy, the related indenyl ligands **4a–c** were obtained from indenyldiphenylphosphine[34] and aryl azides, complete reactions only requiring 2 h at room temperature in this case (Scheme 2). ^{31}P NMR characterization of the crude reaction mixtures revealed more complicate situations than those encountered for the fluorenyl ligands **2a–c**, three isomeric forms **4**, **4′**, and **4″** being detected for each ligand. The preparation of indenyldiphenylphosphine from indenyllithium and chlorodiphenylphosphine is known to give first the allyl isomer **3′** that slowly rearranges to the more stable vinyl isomer **3** at ambient temperature.[34] From a practical viewpoint, complete tautomerization, which can be promoted by filtration through a short pad of alumina[34] or stirring with a catalytic amount of triethylamine, proved to facilitate the workup and isolation of **3** (white solid, 59% yield). But whatever the isomeric ratio **3/3′** engaged, the Staudinger reaction led in all cases to the same isomeric distribution of **4**, **4′**, and **4″**. According to ^1H and ^{13}C NMR spectroscopy, the three isomers could be authenticated as the vinyl phosphazene **4**, the allyl phosphazene **4′**, and the *P*-amino phosphorus ylide **4″**. The vinyl phosphazene form **4**, which has been structurally authenticated in the solid state for **4b**,[33] is generally predominant.[35] It is characterized by a C_q doublet signal at ∼139 ppm ($^1J_{CP} \approx 94$ Hz) attributed to C1 and a broad signal at ∼3.00 ppm in the ^1H NMR associated with a doublet at ∼39.5 ppm ($^2J_{CP} \approx 12.5$ Hz) in the ^{13}C NMR for the ($C8H_2$) methylene of the indenyl.[33] Comparatively, the allyl phosphazene form **4′** exhibits a doublet at ∼4.85 ppm in the ^1H NMR ($^2J_{HP} \approx 27$ Hz) associated in the ^{13}C NMR with a doublet at ∼56.5 ppm ($^1J_{CP} \approx 65$ Hz) for C1 and a CH singlet at ∼132.5 ppm in ^{13}C NMR for C8. Finally, a broad signal at ∼4.5 ppm in the ^1H NMR supports the assignment of the *P*-amino phosphorus ylide form **4″**. Since all of these isomers were supposed to yield the same product upon metalation, no effort was devoted to their separation and they were used directly as a mixture.

Synthesis and Characterization of Zirconium−Fluorenyl Complexes. Elimination of toluene between the bifunctional ligands **2/4** and tetrabenzylzirconium[36] proved to

(28) For related phosphorus-containing analogues of CpSiN CGCs **A**, see: (a) Brown, S. J.; Gao, X.; Harrison, D. G.; Koch, L.; Spence, R. E. v. H.; Yap, G. P. A. *Organometallics* **1998**, *17*, 5445. (b) Kunz, K.; Erker, G.; Döring, S.; Fröhlich, R. *J. Am. Chem. Soc.* **2001**, *123*, 6181. (c) Kotov, V. V.; Avtomonov, E. V.; Sundermeyer, J.; Harms, K.; Lemenovskii, D. A. *Eur. J. Inorg. Chem.* **2002**, 678. (d) Altenhoff, G.; Bredeau, S.; Erker, G.; Kehr, G.; Kataeva, O.; Fröhlich, R. *Organometallics* **2002**, *21*, 4084. (e) Bourissou, D.; Freund, C.; Martin-Vaca, B.; Bouhadir, G. *C. R. Chimie* **2006**, *9*, 1120.

(29) Baiget, L.; Bouslikhane, M.; Escudié, J.; Cretiu Nemes, G.; Silaghi-Dumitrescu, I.; Silaghi-Dumitrescu, L. *Phosphorus, Sulfur, Silicon* **2003**, *178*, 1949.

(30) (a) Murata, S.; Abe, S.; Tomioka, H. *J. Org. Chem.* **1997**, *62*, 3055. (b) Spencer, L. P.; Altwer, R.; Wei, P.; Gelmini, L.; Gauld, J.; Stephan, D. W. *Organometallics* **2003**, *22*, 384.

(31) The opposite situation was encountered in the related $Cp'PMe_2NAd$ ligand.[18]

(32) The following atom numbering has been used in NMR assignment and in X-ray labeling of the $(FluPPh_2NAr)$/$(IndPPh_2NAr)$ ligands and ensuing zirconium complexes:

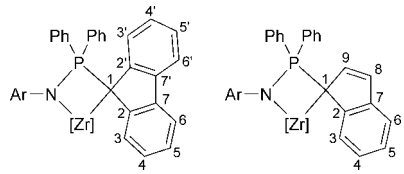

(33) See the Supporting Information.

(34) Falls, K. A.; Anderson, G. K.; Rath, N. P. *Organometallics* **1992**, *11*, 885.

(35) The relative proportions of the three tautomeric structures were estimated by ^{31}P NMR as follows: **4a/4″a/4″a** = 45/14/41, **4b/4′b/4″b** = 82/12/6 and **4c/4′c/4″c** = 57/11/32.

(36) Compared with the conventional salt elimination synthetic route, the toluene elimination strategy greatly facilitates the workup and affords direct access to (di)alkyl complexes: (a) van der Linden, A.; Schaverien, C. J.; Meijboom, N.; Ganter, C.; Orpen, A. G. *J. Am. Chem. Soc.* **1995**, *117*, 3008. (b) Chen, Y.-X.; Marks, T. J. *Organometallics* **1997**, *16*, 3649.

Scheme 3. Synthesis of the Fluorenyl Zirconium Complexes 5a and 6c

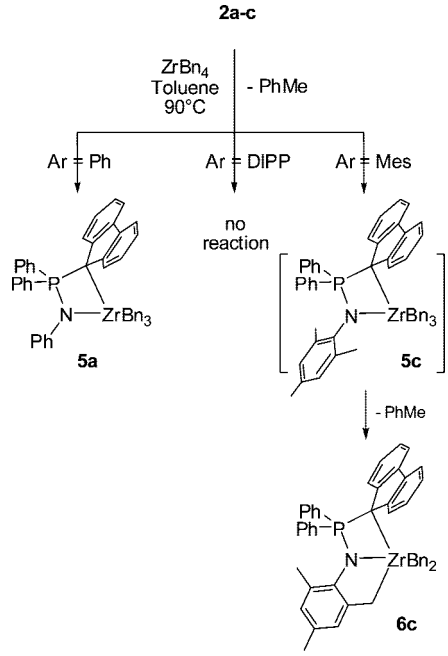

be a convenient way to prepare the corresponding complexes. Accordingly, the reaction of **2a** with 1 equiv of $ZrBn_4$ was complete after 5 h at 90 °C, as indicated by ^{31}P NMR monitoring (Scheme 3). The coordination of a single $(FluPPh_2NPh)^-$ ligand per metal center was deduced from the retention of three benzyl groups in the ^1H NMR spectrum of the resulting complex **5a**. Notably, all of the Flu quaternary carbon atoms appear at more than 130 ppm in ^{13}C NMR, except C1, which resonates at 56.0 ppm as a doublet ($^1J_{PC}$ = 96.6 Hz). This chemical shift is significantly lower than those reported for fluorenyl Zr complexes, even in the rare examples of η^1-coordination (67–88 ppm),[10a,c,12,14] and suggests a rather unusual structure for **5a**.

Complex **5a** proved to be very sensitive to air and moisture. Single crystals, suitable for an X-ray diffraction study, were obtained from a saturated toluene/pentane solution at room temperature. The zirconium center adopts a distorted trigonal bipyramidal geometry in the solid state (Figure 3). Two benzyl groups and the nitrogen occupy the equatorial positions, while the remaining benzyl group and the fluorenyl are located in the pseudoaxial positions. The nitrogen and the C1 atoms of the $(FluPPh_2NPh)^-$ ligand are unsymmetrically bonded to the zirconium center (with Zr−N and Zr−C1 bond lengths of 2.182 and 2.561 Å, respectively), in marked contrast with that found for the corresponding rhodium complex κ^2-N,C[$(FluPPh_2NPh)$Rh(nbd)] (N−Rh 2.123 Å and Rh−C1 2.188 Å),[27] but in a similar way to that observed for the 1-aza-2-phospha(V)allyl complex [$(ArCHPPh_2NMes)Zr(NMe_2)_3$] (Zr−N 2.262 and Zr−C 2.560 Å).[22c] As a result of this chelation, the N−P−C bond angle is rather acute (98.8°) and falls in the typical range of those reported for CGCs **A**. The η^1-Flu coordination is supported by the large distances observed between the remaining Flu carbon atoms and the zirconium center (>3 Å). Although the Zr−C1 bond (2.561 Å) is much longer than that reported for the related complexes **B**[10a,c] (2.28–2.33 Å) and **C**[12] (2.384 Å), the *outward* pyramidalization of C1 ($\Sigma C1_\alpha = 349.4°$)[37] suggests a significant C−Zr bonding interaction. Notably, the η^1 coordination of the fluorenyl ligand results also in a very open P−C1−C_g angle (208°). This value is slightly larger than those reported by Miller for the related Si−C1−C_g angle (198–204°) of the sterically expanded η^1 complexes **B**.[10a,c] Note finally that the electron deficiency induced at the metal by the η^1-Flu coordination is at least partially compensated in **5a** by η^2-coordination of one of the benzyl ligands (Zr−C_{ipso}, 2.62 Å, and Zr−CH_2−C_{ipso}, 87.5°). This behavior is also apparent in solution, the most diagnostic parameters being the chemical shifts for H_{ortho} (6.51 ppm) and C_{ipso} (146.1 ppm) together with the $^1J_{CH}$ value (124 Hz) for the CH_2 group.[38,39] The structure adopted by **5a** confirms further the propensity of the pendent phosphazene moiety to enforce η^1-Flu coordination evidenced for the related rhodium complex,[27] thereby giving access to geometrically constrained and sterically expanded complexes even with group 4 metals.

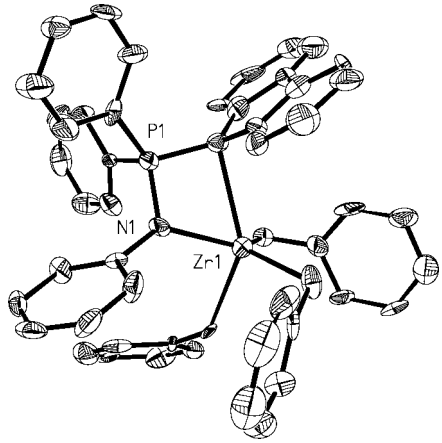

Figure 3. Molecular view of **5a** in the solid state, with hydrogen atoms omitted.

Aiming at probing the influence of the substituent at nitrogen, the coordination of the related ligands **2b** and **2c** was then investigated. No signal other than that of **2b** was detected by ^{31}P NMR spectroscopy after heating for 3 days at 90 °C with 1.7 equiv of $ZrBn_4$, and only thermal decomposition[36b] of the zirconium precursor was observed by ^1H NMR. In contrast, the reaction indeed took place with the less sterically demanding ligand **2c**, although significantly harsher conditions than those used for **2a** were necessary to achieve complete ligand conversion (1.7 vs 1 equiv of $ZrBn_4$ and 5 days vs 5 h at 90 °C). ^{31}P NMR indicated a similar deshielding upon metalation of **2c** ($\Delta\delta$ = 16.8 ppm) than that observed for **2a** ($\Delta\delta$ = 13.5 ppm). However, the ^1H NMR spectrum revealed that only two benzyl groups have been retained, ruling out the formation of the expected complex **5c**. Moreover, only two singlet signals, integrating for three protons each, were observed for the methyl groups at mesityl (2.30 and 2.08 ppm), with an additional singlet signal integrating for only two protons and appearing at higher field (1.80 ppm). These data suggested that another elimination of toluene had occurred between a benzyl group at zirconium and one of the o-methyl groups at mesityl. So far, the poor stability of complex **6c** did not allow us to obtain single crystals

(37) The ylidic carbon center is planar in fluorenylidenephosphoranes: (a) Burford, N.; Clyburne, J. A. C.; Sereda, S. V.; Cameron, T. S.; Pincock, J. A.; Lumsden, M. *Organometallics* **1995**, *14*, 3762. (b) Brady, E. D.; Hanusa, T. P.; Pink, M.; Young , V. G., Jr. *Inorg. Chem.* **2000**, *39*, 6028.

(38) At room temperature, a single set of resonances is observed for the three benzyl groups as a result of fast exchange between the η^1 and η^2-coordination modes.

(39) The coordination mode of benzyl groups toward group 4 metals can usually be distinguished by ^1H and ^{13}C NMR spectroscopy. Typically, η^1-coordination is associated with δ H_{ortho} > 6.5 ppm, δ C_{ipso} ~ 150 ppm, and $^1J_{CH}$ values ~ 120 Hz, while η^2-coordination is associated with δ H_{ortho} < 6.5 ppm, δ C_{ipso} ~ 140 ppm, and $^1J_{CH}$ values ~ 135 Hz. See: Bei, X.; Swenson, D. C.; Jordan, R. F. *Organometallics* **1997**, *16*, 3282 and references therein.

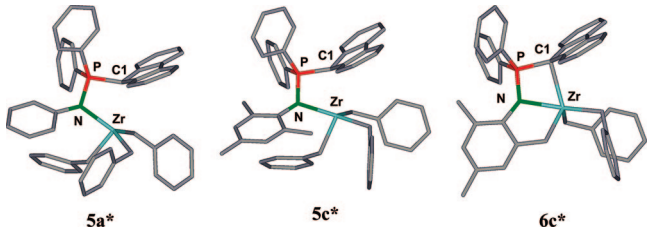

Figure 4. Optimized structures for complexes **5a**,**c*** and **6c*** at the B3PW91/SDD(Zr,P),6-31G**(other atoms) level of theory, with hydrogen atoms omitted.

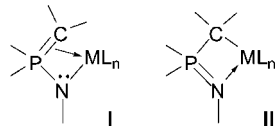

Figure 5. Limiting structures for κ^2-N,C complexes deriving from 1-aza-2-phospha(V)allyl ligands.

Scheme 4. Postulated Assistance of the Phosphazene Sidearm to the Metalation Reaction

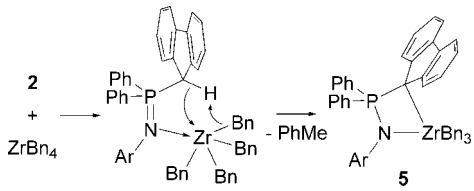

to carry out an X-ray diffraction analysis, but its structure was further assessed by in situ NMR spectroscopy. As far as the hapticity of the fluorenyl ring is concerned, the ^{13}C NMR signal observed at 57.6 ppm ($^1J_{PC}$ = 100.6 Hz) for C1 supported η^1 coordination, by analogy with that observed for **5a**. In addition, the low chemical shifts observed for H_{ortho} (5.94 ppm) and C_{ipso} (142.3 ppm) together with the high $^1J_{CH}$ value (130 Hz) for the CH_2 group suggested an even greater contribution of η^2-coordination for the benzyl coligands than that found in **5a**. From a mechanistic viewpoint, complex **6c** most probably results from the transient formation of **5c** followed by intramolecular CH-activation. ^{31}P NMR monitoring of the reaction between **2c** and $ZrBn_4$ did not allowed us to detect the intermediate complex **5c**, no reaction occurring below 40 °C and only the direct formation of **6c** being observed at higher temperatures.

In order to rationalize the pronounced influence of the steric demand of the aryl group at nitrogen on the kinetics of the metalation reaction, we propose that the formation of complexes **5** results from initial coordination of the phosphazene moiety of **2** to the metal center,[40] followed by intramolecular CH-activation with toluene elimination, that would be favored by increased basicity of the benzyl groups at zirconium as well as higher acidity of the H atom at the fluorenyl induced by the precoordination (Scheme 4).

Theoretical Study of Zirconium−Fluorenyl Complexes. In order to further support the structures proposed for **5c/6c** and to gain more insight into the bonding situations encountered in these complexes, a theoretical investigation has been carried out at the DFT level of theory. The full substitution pattern of the NPC ligands was conserved in order to take reliably into account electronic and steric factors. Accordingly, the key features of complex **5a** could be very well reproduced (with deviations of only 0.06 Å in the N−Zr bond distance and 0.04 Å in the C−Zr one), indicating the ability of the B3PW91/SDD(Zr,P),6-31G**(other atoms) method in describing such systems (Figure 4, Table 1). An NBO analysis was also carried out on **5a*** to get a better understanding of the unsymmetrical coordination of the NPC skeleton that markedly contrasts with the almost symmetric coordination previously observed for the related rhodium complex. Accordingly, the C−M bond is significantly polarized in **5a*** (90% C1−10% Zr) {vs 35% C1−65% Rh in κ^2-N,C[(FluPPh$_2$NPh)Rh(nbd)]}. The combination of X-ray and NBO analyses thus suggests that the behavior of the chelating (FluPPh$_2$NPh)$^-$ ligand is best described as an amido/phosphorus ylid in **5a** (Lewis structure **I**) and as a phosphazene/alkyl in κ^2-N,C[(FluPPh$_2$NPh)Rh(nbd)] (Lewis structure **II**) (Figure 5).[41]

In addition, a minimum could be located on the potential energy surface (PES) for the putative intermediate **5c***. According to its optimized geometry, complex **5c*** retains the η^1-coordination of the fluorenyl ring and an unsymmetrical bonding of the NPC skeleton. In fact, the key geometric features predicted for complex **5c*** very much resemble those of **5a***, except that none of the benzyl group at zirconium is η^2-coordinated. This subtle difference between **5a*** and **5c*** most likely results from the increased steric crowding induced by the mesityl substituent at nitrogen, a situation that also probably favors the intramolecular CH-activation leading to **6c**. The optimized geometry of **6c*** further supports the structure deduced from the spectroscopic analysis, with retention of the η^1-Flu coordination and cyclometalation of one of the ortho positions of the mesityl ring, resulting in a short CH_2−Zr bond (2.24 Å). Notably, the transformation of **5c*** into **6c*** is accompanied by (i) the rotation of the aryl ring at nitrogen by about 90°, (ii) a pseudorotation of the zirconium environment (the pseudoaxial positions being now occupied by the nitrogen atom and one of the remaining benzyl group at zirconium), (iii) a shortened C1−Zr bond (2.54 → 2.46 Å), and (iv) a slight decrease of the steric expansion as measured by the P−C1−C_g bond angle (208 → 201°). The cyclometalation reaction (**5c*** → **6c*** + toluene) is predicted to be favored energetically, with a ΔE value of –7.74 kcal/mol.[42] Although the cyclometalation of phosphazenes is all but unknown, the transformation of **5c** into **6c** deserves some comments. Indeed, cyclometalation reactions of phosphazenes occur usually at a P-substituent (as typically illustrated by complexes of 1-aza-2-phospha(V)allyl ligands[22a–c,23b,c] and ortho-metalated triphenylphosphazenes[43]), but only scarcely at the *N*-substituent.[44] In addition, the formation of **6c** provides a rare example of intramolecular CH-activation within neutral group 4 complexes.[45,46] From a mechanistic viewpoint, the reaction may proceed either by σ-bond metathesis or by α-elimination of toluene leading to a zirconium−benzylidene complex followed by intramolecular addition of a CH bond from an ortho-methyl group at Mes.[45c,d]

(40) For representative examples of phosphazene complexes with group 4 metals, see refs 22b,c.

(41) The contribution of forms **I** and **II** have also been discussed for 1-aza-2-phospha(V)allyl complexes.[22a,23b]

(42) The Free Gibbs energy can hardly be computed for such a large system, but the entropic term for the fragmentation reaction (**5c*** → **6c*** + toluene) can be roughly estimated to favor the cyclometalated complex by 8 ± 2 kcal/mol at 25 °C. Watson, L. A.; Eisenstein, O. *J. Chem. Educ.* **2002**, *79*, 1269.

(43) (a) Wei, P.; Chan, K. T. K.; Stephan, D. W. *Dalton Trans.* **2003**, 3804. (b) Chan, K. T. K.; Spencer, L. P.; Masuda, J. D.; McCahill, J. S. J.; Wei, P.; Stephan, D. W. *Organometallics* **2004**, *23*, 381.

(44) (a) Vicente, J.; Abad, J. A.; Clemente, R.; López-Serrano, J.; Ramírez de Arellano, M. C.; Jones, P. G.; Bautista, D *Organometallics* **2003**, *22*, 4248. (b) Aguilar, D.; Aragüés, M. A.; Bielsa, R.; Serrano, E.; Navarro, R.; Urriolabeitia, E. P. *Organometallics* **2007**, *26*, 3541.

Table 1. Selected Bond Lengths and Angles (in Å and deg, Respectively) for Complexes 5a, 5c, and 6c

	N-Zr	C-Zr	N-Zr-C	N-P	P-C	N-P-C	$\Sigma C1_\alpha$	P-C1-C_g
5a (X-ray)	2.182(6)	2.561(8)	64.9(2)	1.655(6)	1.724(7)	98.8(3)	349.4	204.0
5a[a]	2.24	2.56	65.9	1.67	1.79	98.7	344.8	212.8
5c[a]	2.28	2.54	66.5	1.68	1.79	99.5	348.4	208.1
6c[a]	2.28	2.46	66.7	1.68	1.79	98.5	353.4	201. 1

[a] Predicted at the B3PW91/SDD(Zr,P),6-31G**(other atoms) level of theory.

Scheme 5. Synthesis of the Indenyl Zirconium Complexes 7a–c and 8c

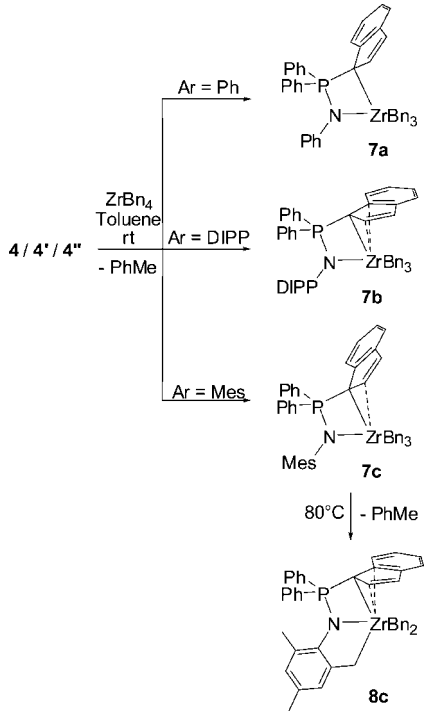

Synthesis and Characterization of Zirconium−Indenyl Complexes. The geometrically constrained and sterically expanded structures evidenced for complexes **5a**,**c** demonstrate the propensity of the phosphazene sidearm to enforce low η^1-fluorenyl coordination even with group 4 metals. This prompted us to investigate the possible access to η^1-indenyl coordination from the corresponding $(IndPPh_2NAr)^-$ ligands. Such η^1-coordination is less favored with indenyl than with fluorenyl rings due to competitive η^2- or η^3-coordination, and with group 4 metals, it has only been structurally authenticated in complexes **D**,[13] **G**,[15] and **H**.[16] Thanks to reduced steric pressure, the phenylated ligand **4a** (engaged as a mixture of its three isomers **4**, **4′**, and **4″**) readily reacted with $ZrBn_4$ (1 equiv) in toluene at room temperature (Scheme 5). According to ^{31}P NMR monitoring, the reaction was complete in a few minutes (<10 min), and all isomers led to a single product **7a** exhibiting a signal at 17.6 ppm. Complex

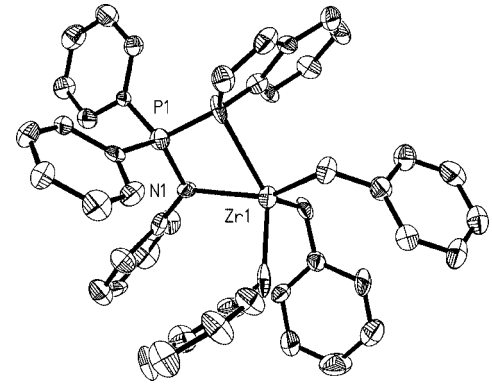

Figure 6. Molecular view of **7a** in the solid state, with hydrogen atoms omitted.

7a proved to be highly unstable in solution at room temperature (noticeable decomposition being typically observed within a few hours)[47] and was therefore characterized by multinuclear NMR at 250 K. The ^1H NMR spectrum revealed the presence of three equivalent benzyl groups per $(IndPPh_2NPh)$ ligand, the CH_2 groups appearing as an AB system (δ 1.89 and 2.02 ppm, $^2J_{HH}$ = 10.5 Hz) as expected because of the dissymmetry induced by the indenyl fragment. The downfield chemical shifts of the remaining protons H8 (7.02 ppm) and H9 (6.57 ppm)[32] of the five-membered ring suggested a low hapticity for the indenyl fragment, a hypothesis which is further supported by the doublet signal observed at 67.8 ppm ($^1J_{PC}$ = 111.4 Hz) in ^{13}C NMR for C1.[48]

Single crystals of **7a**, suitable for an X-ray diffraction study, were obtained from a saturated toluene solution at −20 °C (Figure 6, Table 2). In a similar way to that observed in **5a**, the zirconium center adopts a distorted trigonal bipyramidal geometry (with one of the benzyl groups at zirconium and the nitrogen atom occupying the pseudoaxial positions), and the NPC chelate is unsymmetrically bonded to the metal. All of the benzyl groups are η^1-coordinated, and the distances between zirconium and the carbon atoms of the indenyl C_5-ring are all longer than 2.85 Å, excepted Zr−C1 (2.603 Å). Although the latter value significantly exceeds those observed in complexes **B**−**G** and even in **5a** (2.561 Å), it clearly indicates some bonding interaction. The η^1 coordination of the indenyl ring is accompanied by the *outward* pyramidalization of C1 ($\Sigma C1_\alpha$ = 352.0°), resulting in a widened P−C1−C_g bond angle (202.4°). This result thus confirms the propensity of the pendent phos-

(45) For selected examples of intramolecular activation of C_{sp^2}−H bonds, see: (a) Bulls, A. R.; Schaefer, W. P.; Serfas, M.; Bercaw, J. E. *Organometallics* **1987**, *6*, 1219. (b) Qian, B.; Scanlon, W. J., IV; Smith, M. R., III; Morty, D. H.; *Organometallics* **1999**, *18*, 1693. (c) Shao, P.; Gendron, R. A. L.; Berg, D. J.; Bushnell, G. W. *Organometallics* **2000**, *19*, 509. (d) Deckers, P. J. W.; Hessen, B. *Organometallics* **2002**, *21*, 5564. (e) Planalp, R. P.; Andersen, R. A.; Zalkin, A. *Organometallics* **1983**, *2*, 16. (f) Jimenez Pindado, G.; Thornton-Pett, M.; Bochmann, M. *Chem. Commun.* **1997**, 609. (g) Pool, J. A.; Lobkovsky, E.; Chirik, P. J. *J. Am. Chem. Soc.* **2003**, *125*, 2241–2251. (h) Otten, E.; Dijkstra, P.; Visser, C.; Meetsma, A.; Hessen, B. *Organometallics* **2005**, *24*, 4374. (i) Waterman, R. *Organometallics* **2007**, *26*, 2492.

(46) A zirconocene imido complex was recently found to be capable of intermolecularly activating the C_{sp^3}−H bonds of mesitylene; see: Hoyt, H. M.; Bergman, R. G. *Angew. Chem., Int. Ed.* **2007**, *46*, 5580.

(47) α-Elimination of toluene leading to extremely reactive zirconium−carbene complex seems the most probable decomposition route of **7a**. For rare examples of stable zirconium−benzylidene complexes, see: (a) Fryzuk, M. D.; Duval, P. B.; Mao, S. S. S.; Zaworotko, M. J.; MacGillivray, L. R. *J. Am. Chem. Soc.* **1999**, *121*, 2478. (b) Weng, W.; Yang, L.; Foxman, B. M.; Ozerov, O. V. *Organometallics* **2004**, *23*, 4700.

(48) The high-field shift accompanying the ring slippage from η^5- to η^1-indenyl coordination has been established for late transition metals, especially palladium: (a) Sui-Seng, C.; Enright, G. D.; Zargarian, D. *Organometallics* **2004**, *23*, 1236. (b) Sui-Seng, C.; Enright, G. D.; Zargarian, D. *J. Am. Chem. Soc.* **2006**, *128*, 6508.

Table 2. Selected Bond Lengths and Angles (in Å and deg, Respectively) for Complexes 7a–c and 8c

	N−Zr	C1−Zr	C2−Zr	C9−Zr	C7−Zr	C8−Zr	N−Zr−C	N−P	P−C1	N−P−C	ΣC1$_\alpha$	P−C1−C$_g$	*E*
7a	2.153(6)	2.603(8)	2.875(8)	3.660(8)	3.865(9)	4.257(9)	63.9(2)	1.616(5)	1.743(8)	98.4(4)	352.0	202.4	
7a$_1$[a]	2.22	2.66	2.95	3.66	3.92	4.27	65.6	1.67	1.77	100.2	353	207.1	0
7a$_2$[a]	2.38	2.47	2.75	2.50	2.85	2.66	66.1	1.66	1.79	99.8	357.4	163.5	7.7
7b	2.327(2)	2.513(3)	2.692(3)	2.681(3)	2.953(3)	2.913(3)	64.0(1)	1.616(2)	1.759(3)	99.1(2)	357.5	165.8	
7b$_1$[a]	2.27	2.57	3.15	3.35	3.96	4.04	66.5	1.68	1.78	100.8	353.6	199.9	6.2
7b$_2$[a]	2.38	2.53	2.70	2.69	2.95	2.90	64.1	1.66	1.78	99.0	358.3	158.3	0
7c	2.235(4)	2.535(7)	3.504(7)	2.815(7)	4.055(7)	3.707(7)	64.7(2)	1.623(4)	1.742(6)	99.2(3)	353.6	201.5	
7c$_1$[a]	2.22	2.64	3.15	3.61	4.11	4.33	64.4	1.68	1.78	101.5	350.6	209.8	5.5
7c$_2$[a]	2.37	2.55	2.79	2.69	3.05	2.95	63.9	1.66	1.78	98.6	358.4	158.6	3.1
7c$_3$[a]	2.26	2.61	3.61	2.81	4.17	3.74	64.6	1.67	1.77	99.2	353.1	202.7	0
8c$_1$[a]	2.31	2.55	2.88	2.55	2.97	2.78	65.1	1.65	1.79	99.5	357.3	160.9	0
8c$_2$[a]	2.30	2.51	2.68	2.78	3.03	3.05	65.8	1.65	1.78	99.5	358.5	170.5	0.1

[a] Predicted at the B3PW91/SDD(Zr,P),6-31G**(other atoms) level of theory. *E*, relative energy in kcal/mol.

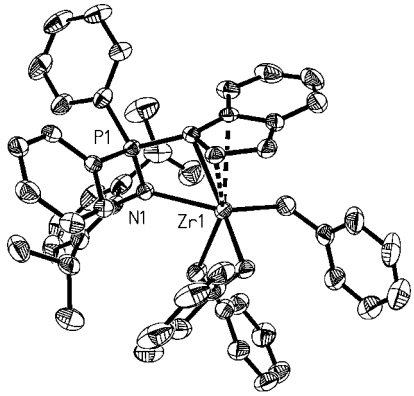

Figure 7. Molecular view of **7b** in the solid state, with hydrogen atoms omitted.

phazene moiety to enforce not only η^1-Flu but also η^1-Ind coordination to group 4 metals, and to the best of our knowledge, complex **7a** is the first geometrically constrained and sterically expanded complex featuring an indenyl ring.

The much higher reactivity of the indenyl (vs fluorenyl) ligand noticed with **4a** (vs **2a**) encouraged us to investigate then the coordination of the more sterically demanding ligands **4b/c** and to determine thereby the influence of the substituent at nitrogen. Accordingly, the reaction of **4b** featuring the DIPP group with 1 equiv of $ZrBn_4$ took place within 10 h at room temperature (whereas no reaction was observed with its fluorenyl analogue **2b** even at 90 °C) to give a new complex **7b** exhibiting a ^{31}P NMR signal at δ 12.6 ppm. The ^1H NMR spectrum indicated the presence of three benzyl groups per ($IndPPh_2NDIPP$) ligand, and the broad ^{13}C NMR signal observed for C1 at 73.5 ppm supported low coordination of the indenyl ring. No additional information could be gained from the NMR data, only broad signals being observed even at low temperature (−50 °C). But the precise structure of complex **7b** could be assessed by crystallization from a THF solution at −20 °C and X-ray diffraction analysis (Figure 7). Accordingly, the distorted trigonal bipyramidal geometry around zirconium was retained, but the steric pressure induced by the DIPP vs phenyl group induced a noticeable elongation of the Zr−N bond (2.327 Å, compared to 2.153 Å in **7a**) and, as a compensation, a shortening of the Zr−C1 distance (2.513 Å, compared to 2.603 Å in **7a**). Notably, two other indenyl carbons (C2 and C9) are located at distances <2.80 Å from the zirconium (2.692 Å and 2.681 Å, respectively) suggesting η^3 rather than η^1 coordination.[49] As a result, the environment around C1 is slightly pyramidalized *inward* rather than *outward* ($\Sigma C1_\alpha = 357.5°$) and the P−C1−C$_g$ angle (165°) significantly closes, while remaining noticeably larger than that of CGCs **A** (∼148°). This result reveals that the steric demand of the substituent at nitrogen may dramatically affect the hapticity of the indenyl ring and thereby the overall geometry of the geometrically constrained complex. Notably, η^3-indenyl coordination has only been scarcely observed in group 4 metallocenes, and in all of the previous examples, the Ind/M bonding involved the three external carbon atoms (C1, C8, and C9).[50] The η^3-coordination through C1, C2, and C9, as observed in **7b**, is rather unusual, and noticeably contrasts with the η^5-coordination systematically observed so far for the related IndSiN CGCs, as revealed by a Cambridge Database search.

With the less encumbered ligand **4c** featuring a Mes group at nitrogen, the reaction toward $ZrBn_4$ is complete after 4 h at room temperature in toluene. In marked contrast with that observed in the fluorenyl series, the ^1H NMR spectrum indicated the retention of three benzyl groups per indenyl and the integrity of the mesityl substituent. The ^{13}C NMR chemical shift for C1 (δ 71.3 ppm with $^1J_{PC} = 118.7$ Hz) is at halfway between those of **7a** and **7b** (67.4 and 73.5 ppm, respectively), suggesting low indenyl coordination but not allowing to discriminate between η^1 and η^3 hapticity. The downfield chemical shifts of the remaining protons H8 and H9 of the five-membered ring (6.97 and 6.92 ppm) also suggest weak if any interactions of the corresponding carbon atoms with the metal center. Cooling a saturated solution of **7c** in toluene at −20 °C yielded orange-brown crystals suitable for X-ray diffraction study (Figure 7). Accordingly, **7c** also adopts a distorted trigonal bipyramidal geometry and the key Zr−N and Zr−C1 bond lengths (2.235 and 2.535 Å, respectively) are in between those observed for **7a** and **7b**, as expected from the intermediate steric demand of the mesityl group compared with the phenyl and DIPP substituents. The distances between the other indenyl carbon atoms and the zirconium center are quite large (>3 Å) except Zr−C9 (2.815 Å) which is at the upper limit to consider a bonding interaction. In addition, complex **7c** also exhibits *outward* pyramidalization of C1 ($\Sigma C1_\alpha = 353.6°$) associated with a widened P−C1−C$_g$ angle (201.5°). All these data indicate η^1-coordination of the indenyl ring (or a strongly unsymmetrical η^2-coordination,[51] taking into account the additional weak interaction between Zr and C9). The electron deficiency induced at the metal center by this low hapticity is at least partially compensated by η^2-coordination of one of the benzyl ligands

(49) The weak contacts of Zr with C2 and C9 do not affect the C1−C2, C1−C9, and C9−C8 bond lengths, with deviations of less than 0.03 Å compared with **7a**.

(50) For an ansa-hafnocene complex featuring an η^3-indenyl ring, see: Christopher, J. N.; Jordan, R. J.; Petersen, J. L.; Young, V. G., Jr. *Organometallics* **1997**, *16*, 3044.

Table 3. Crystallographic Data for Complexes 5a and 7a–c

	5a	7a	7b	7c
empirical formula	$C_{52}H_{44}NPZr$	$C_{58.50}H_{54}$ NPZr	$C_{62}H_{70}NO_2PZr$	$C_{51}H_{48}NPZr$
formula weight	805.07	893.22	983.38	797.09
crystal system	monoclinic	triclinic	monoclinic	orthorhombic
space group	*P*2(1)/c	*P*-1	*P*2(1)/*c*	*P*2(1)2(1)2(1)
a, Å	9.9869(14)	12.8962(12)	12.8193(7)	10.7685(4)
b, Å	18.293(3)	12.9966(10)	19.4797(11)	16.9735(7)
c, Å	22.616(3)	15.1856(12)	21.7493(12)	22.2085(9)
α, deg	90	82.994(5)	90	90
β, deg	101.602(3)	78.340(5)	106.4130(10)	90
γ, deg	90	68.739(5)	90	90
V, Å^3	4047.3(10)	2319.7(3)	5209.8(5)	4059.3(3)
Z	4	2	4	4
density$_{calcd}$, Mg/m^3	1.321	1.279	1.254	1.304
absorp coeff, mm^{-1}	0.348	0.311	0.286	0.346
reflections collected	15744	21119	26086	37507
independent reflections	4873	6368	8802	5763
R1 ($I > 2\sigma(I)$)	0.0687	0.0532	0.0429	0.0454
wR2	0.0970	0.1170	0.0965	0.0758
$(\Delta/r)_{max}$ (e Å^{-3})	0.556 and −0.441	0.333 and −0.367	0.417 and −0.358	0.257 and −0.333

at zirconium, as supported by the short $C_{ipso}-Zr$ distance (2.71 Å) and the acute $Zr-CH_2-C_{ipso}$ bond angle (90.5°).

The milder conditions required for the metalation of **4c** (4 h at rt) compared to **2c** (5 days at 90 °C) thus allowed the isolation of the indenyl complex **7c**, whose fluorenyl analogue **5c** could not be detected. We then explored the propensity of **7c** to similarly undergo another cyclometalation reaction. Accordingly, a toluene solution of **7c** was heated at 80 °C, and complete conversion in a new complex **8c** was achieved after 4 h, according to ^{31}P NMR spectroscopy. The elimination of a second molecule of toluene was indicated by the ^{1}H NMR spectrum. As expected, two AB systems integrating for 2H each were observed for the CH_2 groups of the two remaining benzyl groups. A third AB pattern (δ 2.53 and 2.43 ppm, $^2J_{HH} = 13.8$ Hz) was attributed to the metalated ortho position of the mesityl substituent, the two remaining CH_3 groups resonating as two singlets integrating for 3H each (δ 2.27 and 1.60 ppm). The ^{13}C NMR signal observed at 72.7 ppm ($^1J_{PC} = 127.1$ Hz) for C1 is very similar to those of **7a–c**, in agreement with low indenyl hapticity. In addition, the ^{1}H chemical shifts of H9 (6.27 ppm) and H8 (6.93 ppm), suggests that C9, and eventually C8, interact with the metal. No suitable crystals could be obtained in this case to determine the precise coordination of **8c** in the solid state.

Theoretical Study of Zirconium−Indenyl Complexes. The X-ray diffraction analyses carried out on **7a–c** revealed a rather strong influence of the substituent at nitrogen on the coordination mode of the indenyl ring. To further evidence this trend and to estimate the propensity of a given ligand $(IndPPh_2NAr)^-$ to adopt different coordination modes, DFT calculations were performed on the real complexes **7a–c*** and **8c***. For each complex, at least two minima, corresponding to different indenyl hapticities, were located on the PES (see Figure 9, and Table 2 for key geometric data).

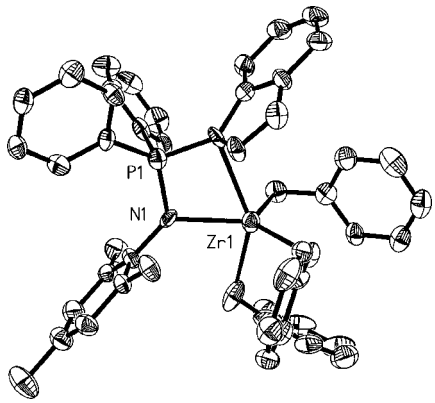

Figure 8. Molecular view of **7c** in the solid state, with hydrogen atoms omitted.

The most stable structure predicted for the *N*-phenylated derivative is the η^1-complex **7a$_1$***, in agreement with experimental observations. The DFT calculations reproduced very well the unsymmetrical coordination of the chelating NPC ligand (N−Zr = 2.22 Å and C1−Zr = 2.66 Å), as well as the *outward* pyramidalization of C1, with a $P-C1-C_g$ bond angle of 207.1°. The second energy minimum located **7a$_2$*** exhibits a much higher indenyl hapticity (with all distances between the metal and the carbon atoms of the five-membered ring varying from 2.47 to 2.85 Å), together with a longer N−Zr bond (2.33 Å). As a consequence, the overall geometry **7a$_2$*** resembles that of CGCs **A**, with an *inward* pyramidalized around C1 associated with a P−C1−Cg angle of 163.5°. The fairly large energy difference predicted between **7a$_1$*** and **7a$_2$*** (7.7 kcal/mol) substantiates the propensity of the phosphazene sidearm to enforce η^1-indenyl coordination.

By analogy with that found experimentally, the related complex **7b*** featuring the DIPP group at nitrogen was predicted to preferentially adopt η^3-indenyl coordination with *inward* pyramidalization around C1. The optimized geometry for the most stable form **7b$_2$*** fits perfectly well with that found in the solid-state. In particular, the elongated N−Zr (2.38 Å) and shortened C1−Zr (2.53 Å) bond distances are nicely reproduced, as well as the additional bonding interactions with C2 (2.70 Å) and C9 (2.69 Å). The related η^1-indenyl structure **7b$_1$*** was found 6.0 kcal/mol higher in energy, as the result of the detrimental steric constrain associated with the shortened N−Zr contact (2.27 Å). Accordingly, the sterically demanding DIPP substituent at nitrogen prevents strong coordination of the phosphazene sidearm and thus disfavors the sterically expanded geometry.

The unsymmetrical η^2-coordination mode and *outward* C1-pyramidalization observed in the solid-state structure of **7c** was also very well reproduced theoretically. This form **7c$_3$*** corre-

(51) For rare examples of η^2-indenyl coordination toward group 4 metals, see: (a) Diamond, G. M.; Green, M. L. H.; Mountford, P.; Popham, N. A.; Chernega, A. N. *Chem. Commun.* **1994**, 103. (b) Diamond, G. M.; Green, M. L. H.; Popham, N. A.; Chernega, A. N. *Chem. Commun.* **1994**, 727. (c) Chen, E. Y.-X; Jin, J. *Organometallics* **2002**, *21*, 13.

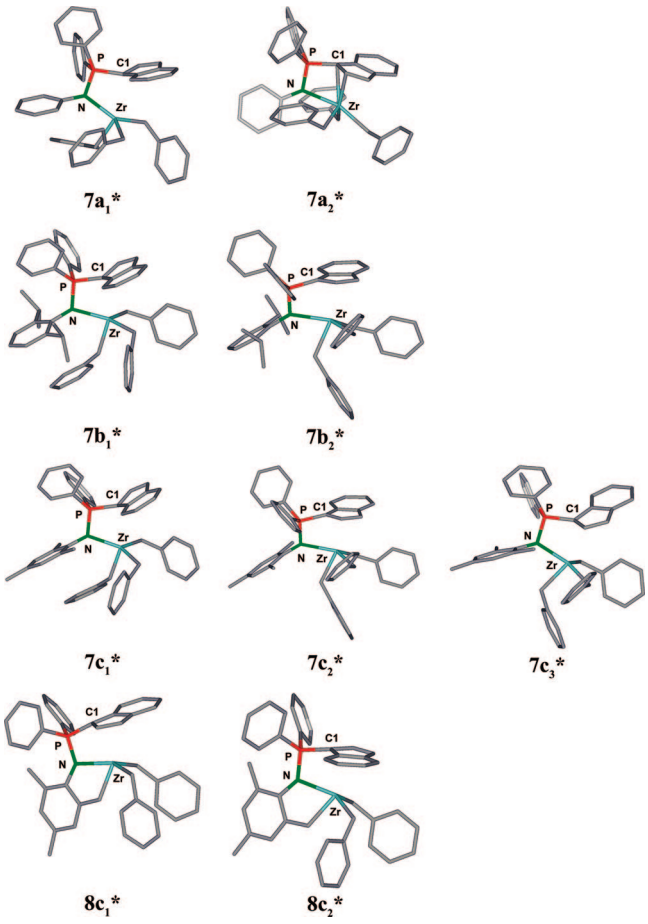

Figure 9. Optimized structures for complexes **7a–c*** and **8c*** at the B3PW91/SDD(Zr,P),6–31G**(other atoms) level of theory, with hydrogen atoms omitted.

sponds to the global mininum on the PES, and the related η^1 and η^3-complexes, **7c₁*** and **7c₂***, were found only 5.5 and 3.1 kcal/mol higher in energy, respectively. Given the results obtained for **7a*** and **7b*** featuring Ph and DIPP groups, respectively, it is logical that the intermediate steric demand of the Mes substituent induces only small energetic separations between the different forms of **7c***.

Calculations were also performed on the ensuing doubly cyclometalated complex **8c** in order to substantiate further the structure suggested by the NMR data. Two energy minima **8c₁*** and **8c₂*** of similar energy (ΔE = 0.1 kcal/mol) were located. For both structures, the intramolecular CH-activation reaction has induced the rotation of the aryl substituent at nitrogen by about 90°, and the cyclometalated ortho position occupies the pseudoaxial position trans to C1. The NPC skeleton is very similarly bonded in the two forms, with a slight elongation of N−Zr bond (2.30 and 2.31 Å) compared to that found in the intermediate complex **7c₃*** (2.26 Å). Moreover, structure **8c₁*** (**8c₂***, respectively) exhibits additional contacts with C9 (2.55 Å) and to a less extent C8 (2.78 Å) [*C*2 (2.68 Å) and C9 (2.78 Å), respectively]. Accordingly, both forms **8c₁*** and **8c₂*** present *inward* pyramidalization around C1 and may be considered η^2- or η^3-coordinated. This situation contrasts with the η^1-coordination and *outward* pyramidalization predicted for the related fluorenyl complex **6c*** and further illustrates the lower propensity of Ind vs Flu rings to adopt η^1-coordination. Finally, the cyclometalation reaction (**7c₃*** → **8c₁*** + toluene) is predicted to be favored energetically, with a ΔE value (−3.38 kcal/mol) in the same range than that computed for the related fluorenyl complexes. This emphasizes the prominent role of kinetic factors in the isolation of the intermediate complex **7c** in the indenyl series.

Conclusion

Bifunctional ligands featuring a phosphazene group directly bonded to a fluorenyl or indenyl ring have been prepared and coordinated to the $ZrBn_3$ fragment via toluene elimination. Despite the associated geometry constraint, the nitrogen atom was found to strongly interact with the metal center and to enforce thereby low fluorenyl and indenyl hapticities. In particular, the η^1-fluorenyl and indenyl complexes **5a** and **7a** were obtained from the ($FluPPh_2NPh$) and ($IndPPh_2NPh$) ligands, respectively. These complexes exhibit *outward* pyramidalization of C_{ipso} (associated with $P-C_{ipso}-C_g$ bond angles of more than 200°), a situation that markedly contrasts with that observed in classical CGCs. These results demonstrate that geometrically constrained and sterically expanded arrangements can be enforced electronically in group 4 metal complexes using a short and strongly donating phosphazene sidearm. In addition, the steric demand of the substituent at nitrogen was shown to strongly influence the indenyl hapticity (from η^1 with Ph, to strongly unsymmetrical η^2 with Mes, and η^3 with DIPP). Original intramolecular CH-activation reactions leading to doubly cyclometalated complexes have also been evidenced upon thermolysis of the NMes-substituted systems.

The development of an increasing variety of geometrically constrained and sterically expanded complexes should greatly help in rationalizing and improving further the peculiar activity and selectivity evidenced by Miller et al. for the prototypical complexes [($FluSiMe_2N$-*t*-Bu)MX_2L] **B** toward homo- and copolymerization of α-olefins.[10] Future research will seek particularly to increase the stability of such complexes by varying the ligand framework as well as the metal fragment so that their reactivity can be investigated and the precise role of low Flu and Ind hapticities can be understood.

Experimental Section

All reactions were performed using standard Schlenk techniques under an argon atmosphere. ^{31}P, ^1H, and ^{13}C spectra were recorded on Bruker Avance 300 or 400 and AMX500 spectrometers. ^{31}P, ^1H, and ^{13}C chemical shifts are expressed with a positive sign, in parts per million, relative to external 85% H_3PO_4 and Me_4Si. Unless otherwise stated, NMR was recorded at 293 K. THF, diethyl ether, and toluene were dried under sodium and distilled prior to use. All organic reagents were obtained from commercial sources and used as received. $ZrBn_4$ was purchased from Strem Chemicals, stocked out of light in a glovebox, and used without further purification. The fluorenyldiphenylphosphine **1**,[29] ensuing phenylphosphazene **2a**,[27] indenyldiphenylphosphine **3**,[34] and azides[30] were prepared according to literature procedures. All of the zirconium complexes proved to be too sensitive to get satisfactory elemental analysis or HRMS data.

Synthesis of $Ph_2FluP{=}N(i\text{-}Pr_2)_2C_6H_3$ (2b). A degassed solution of 2,6-*i*-$Pr_2C_6H_3N_3$ (0.60 g, 3.10 mmol) in toluene (8 mL) was added at room temperature to a degassed suspension of Ph_2PFlu (1.00 g, 2.85 mmol) in toluene (20 mL). After the mixture was stirred for 20 h at 30 °C, the solvent was eliminated under vacuum to yield a pale yellow solid which was washed with cold pentane (20 mL). Yield: 1.20 g (80%). $^{31}P\{^1H\}$ NMR (81 MHz, C_6D_6): δ_{ppm} −1.9 (s). ^1H NMR (300 MHz, C_6D_6): δ_{ppm} 7.64 (d, $^3J_{H,H}$ = 7.8 Hz, 2H, $H_{3,3'}$), 7.46–7.38 (m, 6H, H_{13} and $H_{6,6'}$), 7.18 (m, 2H, H_{10}), 7.10 (m, 2H, $H_{5,5'}$), 7.04 (m, 3H, $H_{4,4'}$ and H_{11}), 6.92–6.78 (m, 6H, H_{15} and H_{14}), 5.20 (d, $^2J_{H,P}$ = 24.6 Hz, 1H, H_1), 3.58 (sept, $^3J_{H,H}$ = 6.8

Hz, 2H, C*H*$(CH_3)_2$), 1.17 (d, $^3J_{H,H}$ = 6.8 Hz, 12H, CH(C*H*$_3)_2$). $^{13}C\{^1H\}$ NMR (75.5 MHz, C_6D_6): δ_{ppm} 144.6 (C_8), 142.4 (d, $^2J_{C,P}$ = 7.4 Hz, C_9), 142.2 (d, $^3J_{C,P}$ = 4.8 Hz, $C_{7,7'}$), 140.2 (d, $^3J_{C,P}$ = 3.9 Hz, $C_{2,2'}$), 131.9 (d, $^2J_{C,P}$ = 8.3 Hz, C_{13}), 131.0 (d, $^4J_{C,P}$ = 2.8 Hz, C_{15}), 128.0 (d, $^1J_{C,P}$ = 91.6 Hz, C_{12}), 127.7 (d, $^3J_{C,P}$= 11.4 Hz, C_{13}), 127.4 (d, $^5J_{C,P}$ = 2.0 Hz, $C_{5,5'}$), 126.5 (d, $^3J_{C,P}$ = 1.9 Hz, $C_{3,3'}$), 126.3 (d, $^4J_{C,P}$ = 2.3 Hz, 6 $C_{4,4'}$), 122.9 (d, $^4J_{C,P}$ = 1.8 Hz, C_{10}), 119.8 (d, $^5J_{C,P}$ = 2.9 Hz, C_{11}), 119.6 (d, $^4J_{C,P}$ = 1.1 Hz, $C_{6,6'}$), 53.4 (d, $^1J_{C,P}$ = 68.7 Hz, C_1), 28.8 (CH), 23.9 (CH_3). MS (EI 78 eV) *m/z*: 483 $(M)^+$, 318 $(M - Flu)^+$, 240 $(M - Flu - Ph)^+$, 165 $(Flu)^+$. Mp: 186 °C. Anal. Calcd for $C_{37}H_{36}NP$: C, 84.54; H, 6.90; N, 2.66. Found: C, 84.14; H, 7.04; N, 2.64.

Synthesis of Ph_2FluP═NMes (2c). A degassed solution of $MesN_3$ (1.00 g, 6.20 mmol) in toluene (5 mL) was added at room temperature to a degassed suspension of Ph_2PFlu (2.15 g, 6.15 mmol) in toluene (50 mL). After the mixture was stirred for 24 h at room temperature, the solvent was eliminated under vacuum to yield a pale yellow solid. Cooling a solution of **2c** in toluene/pentane to −25 °C yielded 2.50 g of pale yellow crystals (84%). $^{31}P\{^1H\}$ NMR (81 MHz, C_6D_6): δ_{ppm} −1.7 (s). ^1H NMR (300 MHz, C_6D_6): δ_{ppm} 7.65 (d, $^3J_{H,H}$ = 7.8 Hz, 2H, $H_{3,3'}$), 7.44 (m, 4H, H_{13}), 7.37 (d, $^3J_{H,H}$ = 7.5 Hz, 2H, $H_{6,6'}$), 7.14 (m, 2H, $H_{5,5'}$), 7.03 (m, 2H, $H_{4,4'}$), 6.95 (m, 2H, H_{15}), 6.90 (m, 4H, H_{14}), 6.85 (m, 2H, H_{10}), 5.12 (d, $^2J_{H,P}$ = 24.0 Hz, 1H, H_1), 2.35 (d, $^5J_{H,H}$ = 1.5 Hz, 6H, *o*-CH_3), 2.25 (d, $^7J_{H,H}$ = 2.4 Hz, 3H, *p*-CH_3). $^{13}C\{^1H\}$ NMR (75.5 MHz, C_6D_6): δ_{ppm} 145.4 (C_8), 142.2 (d, $^2J_{C,P}$ = 4.5 Hz, $C_{7,7'}$), 140.2 (d, $^3J_{C,P}$ = 3.8 Hz, $C_{2,2'}$), 131.9 (d, $^2J_{C,P}$ = 8.3 Hz, C_{13}), 131.6 (d, $^3J_{C,P}$ = 6.8 Hz, $C_{9,9'}$), 130.8 (d, $^4J_{C,P}$ = 3.0 Hz, C_{15}), 129.9 (C_{11}), 129.2 (d, $^1J_{C,P}$ = 92.1 Hz, C_{12}), 128.7 (d, $^4J_{C,P}$ = 2.3 Hz, C_{10}), 127.5 (d, $^3J_{C,P}$=10.6 Hz, C_{14}), 127.2 (d, $^5J_{C,P}$ = 2.3 Hz, $C_{5,5'}$), 126.8 (d, $^3J_{C,P}$ = 3.0 Hz, $C_{3,3'}$), 126.3 (d, $^4J_{C,P}$ = 2.3 Hz, $C_{4,4'}$), 119.5 (d, $^4J_{C,P}$ = 1.5 Hz, $C_{6,6'}$), 53.0 (d, $^1J_{C,P}$ = 65.7 Hz, C_1), 21.6 (d, $^4J_{C,P}$ = 1.5 Hz, *o*-CH_3), 20.5 (d, $^6J_{C,P}$ = 0.8 Hz, *p*-CH_3). MS (EI 70 eV) *m/z*: 483 $(M)^+$, 318 $(M - Flu)^+$, 240 $(M - Flu - Ph)^+$, 165 $(Flu)^+$. Anal. Calcd foror $C_{34}H_{30}NP$: C, 84.45; H, 6.25; N, 2.90. Found: C, 84.21; H, 6.26; N, 2.82. Mp 182 °C.

Synthesis of Ph_2IndP═NPh (4a). A degassed solution of PhN_3 (0.800 g, 6.70 mmol) in dichloromethane (5 mL) was added at room temperature to a degassed solution of Ph_2PInd (2.00 g, 6.60 mmol) in dichloromethane (10 mL). After being stirred for 2 h, the reaction mixture was concentrated (about 10 mL), and pentane (40 mL) was added. The yellow precipitate was filtered off and washed with three portions of pentane (20 mL) to give **4a** as a yellow powder (2.31 g, 90%). $^{31}P\{^1H\}$ NMR (121.4 MHz, C_6D_6): isomer **4a** δ_{ppm} −8.3; isomer **4′a** δ_{ppm} −4.5; isomer **4″a** δ_{ppm} 18.7. ^1H NMR (300 MHz, C_6D_6): isomer **4a** δ_{ppm} 7.90 ppm (m, $^4J_{H,P}$ = 9.8 Hz, 4H, H_{16}), 7.74 (m, 1H, H_3), 7.32 (m, 2H, H_{11}), 7.17 (m, 2H, H_{12}), 7.15 (overlapped, 1H, H_6), 7.05–6.95 (m, 6H, $H_{15,17}$), 7.00 (overlapped, 1H, $H_{4\ or\ 5}$), 6.90 (overlapped, 1H, $H_{4\ or\ 5}$), 6.80 (m, 1H, H_{13}), 6.71 (dt, 1H, $^3J_{H,P}$ = 9.5 Hz, $^3J_{H,H}$ = 1.8 Hz, H_9), 2.98 (pseudo t, 2H, $^4J_{H,P}$ < 2.0 Hz, $^3J_{H,H}$ < 1.8 Hz, H_8); isomer **4″a** δ_{ppm} 4.97 (br s, 1H, N*H*). $^{13}C\{^1H\}$ NMR (75.5 MHz, C_6D_6): isomer **4a** δ_{ppm} 152.0 (d, $^2J_{C,P}$ = 2.1 Hz, C_{10}), 148.4 (d, $^2J_{C,P}$ = 9.4 Hz, C_9), 143.9 (d, $^3J_{C,P}$ = 9.9 Hz, C_7), 143.0 (d, $^2J_{C,P}$ = 11.5 Hz, C_2), 137.6 (d, $^1J_{C,P}$ = 95.6 Hz, C_1), 132.2 (d, $^3J_{C,P}$ = 9.8 Hz, C_{16}), 131.7 (d, $^1J_{C,P}$ = 103.0 Hz, C_{14}), 128.5 (d, $^4J_{C,P}$ = 12.8 Hz, C_{17}), 128.4 (d, $^2J_{C,P}$ = 12.0 Hz, C_{15}), 126.7 ($C_{4\ or\ 5}$), 125.6 ($C_{4\ or\ 5}$), 123.9 (d, $^3J_{C,P}$ = 4.0 Hz, C_3), 123.4 (d, $^4J_{C,P}$ = 3.5 Hz, C_6), 39.7 (d, $^3J_{C,P}$ = 12.9 Hz, C_8). MS (EI, 70 eV) *m/z*: 391 $[M]^+$ (55), 276 $[M - Ind]^+$ (100), 115 $[Ind]^+$ (38); HRMS (ES^+): calcd for $C_{27}H_{22}NP$ 392.1568, found 392.1545. Mp: 105 °C dec.

Synthesis of Ph_2IndP═N(*i*-$Pr_2)_2C_6H_3$ (4b). A degassed solution of (*i*-$Pr_2)_2C_6H_3N_3$ (0.40 g, 2.00 mmol) in dichloromethane (5 mL) was added at room temperature to a degassed solution of Ph_2PInd (0.54 g, 1.80 mmol) in dichloromethane (10 mL). After being stirred for 2 h, the orange solution was evaporated to dryness. The residue was washed with four portions of pentane (5 mL) to yield **4b** as an orange powder (0.95 g, 91%). $^{31}P\{^1H\}$ NMR (121.4 MHz, C_6D_6): isomer **4b** δ_{ppm} −16.5; isomer **4′b** δ_{ppm} −6.0; isomer **4″b** δ_{ppm} 23.9. ^1H NMR (300 MHz, C_6D_6): isomer **4b** δ_{ppm} 7.82–7.75 (m, $^4J_{H,P}$ = 9.6 Hz, 4H, H_{16}), 7.68 (m, 1H, H_3), 7.21–7.17 (m, 3H, $H_{12,13}$), 7.20 (overlapped, 1H, H_6), 7.10–6.97 (m, 6H, $H_{15,17}$), 7.05–6.97 (m, 2H, $H_{4,5}$), 6.29 (dt, 1H, $^3J_{H,P}$ = 9.0 Hz, $^3J_{H,H}$ = 2.0 Hz, H_9), 3.66 (sept, 2H, $^3J_{H,H}$ = 6.9 Hz, −C*H*$(CH_3)_2$), 2.94 (pseudo t, 2H, $^4J_{H,P}$ = 2.0 Hz, $^3J_{H,H}$ = 2.0 Hz, H_8), 0.96 (d, 12H, $^3J_{H,H}$ = 6.9 Hz, −CH(C*H*$_3)_2$); isomer **4′b** δ_{ppm} 6.90 (overlaps, 1H, H_8), 6.55 (br s, 1H, H_9), 4.87 (d, 1H, $^2J_{H,P}$ = 27.1 Hz, H_1), 3.66 (overlaps, 1H, −C*H*$(CH_3)_2$), 3.27 (m, 1H, −C*H*$(CH_3)_2$), 1.26 (d, 6H, $^3J_{H,H}$ = 6.8 Hz, −CH(C*H*$_3)_2$), 0.74 (d, 6H, $^3J_{H,H}$ = 6.8 Hz, −CH(C*H*$_3)_2$); isomer **4″b** δ_{ppm} 4.15 (br s, 1H, N-*H*), 3.80 (br m, 1H, −C*H*$(CH_3)_2$), 3.66 (overlaps, 1H, −C*H*$(CH_3)_2$), 1.06 (overlaps, 6H, −CH(C*H*$_3)_2$), 0.85 (d, 6H, $^3J_{H,H}$ = 6.7 Hz, −CH(C*H*$_3)_2$). $^{13}C\{^1H\}$ NMR (75.5 MHz, C_6D_6): isomer **4b** δ_{ppm} 145.8 (d, $^2J_{C,P}$ = 8.8 Hz, C_9), 144.3 (d, $^2J_{C,P}$ = 2.7 Hz, C_{10}), 143.8 (d, $^3J_{C,P}$ = 9.5 Hz, C_7), 143.3 (d, $^2J_{C,P}$ = 11.6 Hz, C_2), 142.8 (d, $^3J_{C,P}$ = 7.0 Hz, C_{11}), 140.7 (d, $^1J_{C,P}$ = 95.1 Hz, C_1), 132.1 (d, $^1J_{C,P}$ = 106.0 Hz, C_1), 132.0 (d, $^3J_{C,P}$ = 9.6 Hz, C_{16}), 131.1 (d, $^4J_{C,P}$ = 2.7 Hz, C_{17}), 128.3 (d, $^2J_{C,P}$ = 12.1 Hz, C_{15}), 126.4 ($C_{4\ or\ 5}$), 125.5 ($C_{4\ or\ 5}$), 123.5 (d, $^3J_{C,P}$ = 9.8 Hz, C_3), 122.8 (d, $^4J_{C,P}$ = 2.5 Hz, C_{12}), 119.9 (d, $^5J_{C,P}$ = 2.5 Hz, C_{13}), 39.4 (d, $^3J_{C,P}$ = 12.6 Hz, C_8), 28.5 (*C*H$(CH_3)_2$), 23.6 (CH(*C*H$_3)_2$); isomer **4′b** δ_{ppm} 134.0 (d, $^2J_{C,P}$ = 8.7 Hz, C_9), 132.4 (d, $^3J_{C,P}$ = 9.5 Hz, C_8), 56.8 (d, $^1J_{C,P}$ = 67.9 Hz, C_1), 28.9 (*C*H$(CH_3)_2$), 28.1 (*C*H$(CH_3)_2$), 23.8 (CH(*C*H$_3)_2$), 23.7 (CH(*C*H$_3)_2$); isomer **4″b** δ_{ppm} 28.9 (*C*H$(CH_3)_2$), 28.1 (*C*H$(CH_3)_2$), 23.8 (CH(*C*H$_3)_2$), 23.7 (CH(*C*H$_3)_2$). MS (EI, 70 eV) *m/z*: 475 $[M]^+$ (74), 460 $[M - CH_3]^+$ (28), 432 $[i\text{-}Pr]^+$ (40), 360 $[M - Ind]^+$ (75), 300 $[M - N((i\text{-}Pr_2)_2C_6H_3)]^+$ (12), 185 $[M - N((i\text{-}Pr_2)_2C_6H_3) - Ind]^+$ (72), 115 $[Ind]^+$ (85); HRMS (ES^+): calcd for $C_{33}H_{35}NP$ 476.2507, found 476.2498. Mp: 175 °C dec.

Synthesis of Ph_2IndP═NMes (4c). A degassed solution of $MesN_3$ (0.61 g, 3.80 mmol) in dichloromethane (5 mL) was added at room temperature to a degassed solution of Ph_2PInd (0.96 g, 3.20 mmol) in dichloromethane (10 mL). After being stirred for 2 h, the reaction mixture was concentrated (about 5 mL), and pentane (60 mL) was added to induce the precipitation of a black-orange solid. The orange solution was filtered and evaporated to dryness. The orange residue was washed with pentane (3 × 10 mL), and **4c** was obtained as a yellow powder (0.95 g, 68%). $^{31}P\{^1H\}$ NMR (121.4 MHz, C_6D_6): isomer **4c** δ_{ppm} −18.2; isomer **4″c** δ_{ppm} 22.3; isomer **4′c** δ_{ppm} −5.4. ^1H NMR (300 MHz, C_6D_6): isomer **4c** δ_{ppm} 7.82–7.77 (m, 4H, H_{16}), 7.68 (dd, 1H, $^3J_{H,P}$ = 6.3 Hz, $^3J_{H,H}$ = 2.0 Hz, H_3), 7.17 (overlaps, 1H, H_6), 7.06–6.96 (m, 6H, $H_{15,17}$), 6.96–6.91 (m, 2H, $H_{4,5}$), 6.91 (br s, 2H, H_{12}), 6.41 (dt, 1H, $^3J_{H,P}$ = 9.2 Hz, $^3J_{H,H}$ = 1.6 Hz, H_9), 3.00 (br s, 2H, H_8), 2.30 (s, 9H, CH_3), **isomer 4′c** δ_{ppm} 4.88 (d, 1H, $^2J_{H,P}$ = 26.7 Hz, H_1), 2.30 (s, 6H, *o*-CH_3), 2.26 (overlaps, 3H, *p*-CH_3); isomer **4″c** δ_{ppm} 4.00 (br s, 1H, N*H*), 2.00 (s, 3H, *p*-CH_3), 1.74 (s, 3H, *o*-CH_3). $^{13}C\{^1H\}$ NMR (75.5 MHz, C_6D_6): isomer **4c** δ_{ppm} 145.5 (d, $^2J_{C,P}$ = 8.8 Hz, C_9), 144.9 (d, $^2J_{C,P}$ = 1.6 Hz, C_{10}), 143.8 (d, $^3J_{C,P}$ = 9.5 Hz, C_7), 143.4 (d, $^2J_{C,P}$ = 11.7 Hz, C_2), 141.1 (d, $^1J_{C,P}$ = 94.2 Hz, C_1), 138.0 (d, $^3J_{C,P}$ = 2.6 Hz, C_{11}), 131.9 (d, $^3J_{C,P}$ = 9.7 Hz, C_{16}), 130.9 (d, $^4J_{C,P}$ = 2.7 Hz, C_{17}), 128.8 (d, $^4J_{C,P}$ = 2.6 Hz, C_{12}), 128.2 (d, $^2J_{C,P}$ = 12.1 Hz, C_{15}), 126.4 ($C_{4\ or\ 5}$), 125.4 ($C_{4\ or\ 5}$), 123.6 (C_3 and C_6), 39.4 (d, $^3J_{C,P}$ = 12.5 Hz, C_8), 20.9 (*o*-CH_3), 20.6 (*p*-CH_3); isomer **4′c** δ_{ppm} 56.3 (d, $^1J_{C,P}$ = 63.2 Hz, C_1), 21.3 (*o*-CH_3), 20.4 (*p*-CH_3); isomer **4″c** δ_{ppm} 70.4 (d, $^1J_{C,P}$ = 140.2 Hz, C_1), 20.6 (*p*-CH_3), 19.6 (*o*-CH_3). MS (EI, 70 eV) *m/z*: 433 $[M]^+$ (87), 318 $[M - Ind]^+$ (100), 115 $[Ind]^+$ (82). HRMS (ES^+): calcd for $C_{30}H_{29}NP$ 434.2038, found 434.2031. Mp: 165 °C dec.

Synthesis of Complex $ZrBn_3$(Ph_2FluP═NPh) (5a). A solution of **2a** (296 mg, 0.67 mmol) and $ZrBn_4$ (307 mg, 0.67 mmol) in toluene was heated at 90 °C in the absence of light for 5 h. The toluene was evaporated under vacuum to yield an orange-brown solid (512 mg, 95%). Orange-brown crystals of **5a** suitable for X-ray

crystallography were obtained from a toluene/pentane solution at room temperature. $^{31}P\{^1H\}$ NMR (121.4 MHz, C_6D_6): δ_{ppm} 21.3 (s). ^1H NMR (300.1 MHz, C_6D_6): δ_{ppm} 8.04 (d, $^3J_{H,H}$ = 7.5 Hz, 2H, $H_{6,6'}$), 7.28–7.08 (m, 10H, $H_{4,4',6,6',9,9',13}$), 7.08–7.00 (m, 11H, $H_{3,3',10,11,19}$), 6.95–6.85 (m, 5H, $H_{15,20}$), 6.80–6.70 (m, 4H, H_{14}), 6.58 (d, $^3J_{H,H}$ = 8.1 Hz, 6H, H_{18}), 2.17 ppm (s, 6H, H_{16}). $^{13}C\{^1H\}$-NMR (75.5 MHz, C_6D_6): δ_{ppm} 146 (C_{17}), 141.3 (d, $^2J_{C,P}$ = 6.5 Hz, $C_{2,2'}$), 137.0 (d, $^3J_{C,P}$ = 10.3 Hz, $C_{7,7'}$), 132.8 (d, $^2J_{C,P}$ = 10.3 Hz, C_{13}), 132.4 (C_{15}), 129.2 ($C_{3,3'}$), 129.1 (d, $^2J_{C,P}$ = 81.0 Hz, C_{12}), 128.8 (d, $^2J_{C,P}$ = 11.8 Hz, C_{14}), 128.2 (C_{19}), 127.9 (C_{18}), 126.3 (C_{10}), 126.1 ($C_{4,4'}$), 123.4 ($C_{5,5'}$), 123.2 ($C_{9,9'}$), 122.3 (C_{20}), 120.8 ($C_{6,6'}$), 120.1 (C_{11}), 79.7 (C_{16}), 56.0 ppm (d, $^2J_{C,P}$ = 96.6 Hz, C_1), C_8 not observed. Mp: 146 °C dec.

Synthesis of Complex 6c. Reaction Performed in an NMR Tube. A solution of **2c** (36 mg, 0.08 mmol) and $ZrBn_4$ (58 mg, 0.13 mmol, 1.7 equiv) in toluene-d_8 (0.75 mL) was heated at 90 °C in the absence of light for 5 days. Complete consumption of the ligand was observed. $^{31}P\{^1H\}$ NMR (81 MHz, toluene-d_8): δ_{ppm} 15.1 (s). ^1H NMR (400 MHz, toluene-d_8): δ_{ppm} 7.98 (d, $^3J_{H,H}$ = 7.8 Hz, 2H, $H_{6,6'}$), 7.52 (m, 4H, H_{13}), 7.18 (m, 2H, $H_{5,5'}$), 7.03 (m, 2H, H_{15}), 6.96 (m, 2H, H_{19}), 6.94 (m, 2H, $H_{4,4'}$), 6.90 (m, 5H, $H_{10,14}$), 6.86 (m, H_{20}), 6.69 (m, 1H, $H_{10'}$), 6.68 (m, 2H, $H_{3,3'}$), 5.94 (d, $^3J_{H,H}$ = 8.0, 4H, H_{18}), 2.30 (s, 3H, *p*-CH_3), 2.08 (s, 3H, *o*-CH_3), 1.80 (s, 2H, CH_2Ar), 1.47 and 1.49 (2 s, 2H each, H_{16}). ^{13}C NMR (100 MHz, toluene-d_8): δ_{ppm} 145.9 (d, $^2J_{C,P}$ = 6.5 Hz, C_8), 144.8 (d, $^3J_{C,P}$ = 15.6 Hz, $C_{9'}$ Ar *ipso*-bridge), 142.3 (C_{17}), 141.8 (d, $^2J_{C,P}$ = 7.8 Hz, $C_{2,2'}$), 136.8 (d, $^3J_{C,P}$ = 10.0 Hz, $C_{7,7'}$), 132.8 (d, $^4J_{C,P}$ = 8.0 Hz, C_{11}), 132.5 (d, $^2J_{C,P}$ = 9.9 Hz, C_{13}), 132.0 (d, $^4J_{C,P}$ = 2.8 Hz, C_{15}), 130.5 (C_{19}), 128.6 (C_{14}), 128.3 (C_{10}), 127.5 ($C_{10'}$), 127.0 ($C_{18,18'}$), 125.3 (d, $^4J_{C,P}$ = 1.2 Hz, $C_{4,4'}$), 125.0 (d, $^3J_{C,P}$ = 1.7 Hz, C_9), 122.8 (C_{20}), 122.5 ($C_{5,5'}$), 121.0 (d, $^3J_{C,P}$ = 1.3 Hz, $C_{3,3'}$), 120.5 ($C_{6,6'}$), 74.5 (C_{16}), 68.7 (CH_2 Ar), 57.6 (d, $^1J_{C,P}$ = 100.6 Hz, C_1), 23.2 (*o*-CH_3), 20.8 (*p*-CH_3).

Synthesis of $ZrBn_3(Ph_2IndP{=}NPh)$ (7a). Reaction performed in an NMR Tube. Compound **4a** (39 mg, 0.1 mmol) and $ZrBn_4$ (46 mg, 0.1 mmol, 1.0 equiv) were dissolved in dichloromethane-d_2 (0.6 mL) at room temperature and manually shaken for a few minutes. Complete consumption of the ligand was observed. Pale yellow-orange crystals of **7a** suitable for X-ray crystallography were obtained from a toluene (1 mL)/pentane (0.4 mL) mixture at 0 °C. $^{31}P\{^1H\}$ NMR (202.5 MHz, CD_2Cl_2, 250 K): δ_{ppm} 17.6. $^1H\{^{31}P\}$ NMR (500 MHz, CD_2Cl_2, 250 K): δ_{ppm} 7.80 (d, 1H, $^3J_{H,H}$ = 7.9 Hz, H_6), 7.67 (m, 2H, H_{17}), 7.44 (m, 4H, H_{16}), 7.40 (overlapped, 1H, H_5), 7.39–7.34 (m, 4H, H_{15}), 7.28 (overlapped, 1H, H_6), 7.22 (m, 2H, H_{12}), 7.15 (pseudo t, 6H, $^3J_{H,H}$ = 8.0 Hz, H_{21}), 7.02 (d, 1H, $^3J_{H,H}$ = 4.6 Hz, H_8), 6.98 (t, 3H, $^3J_{H,H}$ = 7.0 Hz, H_{22}), 6.90 (d, 1H, $^3J_{H,H}$ = 7.9 Hz, H_3), 6.73 (d, 2H, $^3J_{H,H}$ = 7.6 Hz, H_{11}), 6.60 (t, 1H, $^3J_{H,H}$ = 7.9 Hz, H_{13}), 6.57 (d, 1H, $^3J_{H,H}$ = 4.6 Hz, H_9), 6.48 (d, 6H, $^3J_{H,H}$ = 8.0 Hz, H_{20}), 2.02 (d, 3H, $^2J_{H,H}$ = 10.5 Hz, H_{18}), 1.89 (d, 3H, $^2J_{H,H}$ = 10.5 Hz, $H_{18'}$). $^{13}C\{^1H\}$ NMR (125.3 MHz, CD_2Cl_2, 250 K): δ_{ppm} 146.3 (C_{19}), 146.0 (d, $^2J_{C,P}$ = 5.0 Hz, C_{10}), 140.7 (d, $^3J_{C,P}$ = 11.3 Hz, C_7), 134.6 (d, $^2J_{C,P}$ = 10.1 Hz, C_2), 133.3 (d, $^4J_{C,P}$ = 2.5 Hz, C_{17}), 132.8 (d, $^2J_{C,P}$ = 11.0 Hz, C_{15}), 129.7 (d, $^2J_{C,P}$ = 11.3 Hz, C_9), 129.4 (d, $^3J_{C,P}$ = 10,5 Hz, C_{16}), 129.3 (C_{12}), 128.9 (C_{21}), 128.2 (d, $^1J_{C,P}$ = 87.0 Hz, C_{14}), 127.2 (C_{20}), 125.8 (d, $^3J_{C,P}$ = 10.0 Hz, C_{11}), 124.1 (C_4), 124.0 (C_{13}), 123.5 (C_5), 123.2 (C_6), 122.1 (C_{22}), 119.7 (d, $^3J_{C,P}$ = 12.5 Hz, C_8), 118.4 (C_3), 78.4 (C_{18}), 67.8 (d, $^1J_{C,P}$ = 111.4 Hz, C_1).

Synthesis of $ZrBn_3(Ph_2IndP{=}N(i\text{-}Pr_2)C_6H_3)$ (7b). A solution of **4b** (144 mg, 0.30 mmol) and $ZrBn_4$ (194 mg, 0.43 mmol) in toluene (1.5 mL) was stirred at room temperature in the absence of light for 10 h. The solution orange was filtered and placed at 0 °C for 15 h. The yellow precipitate formed was filtered and washed with cold (−20 °C) toluene (2 mL). Compound **7b** was obtained as a pale yellow powder (0.16 g, 64%). Yellow crystals of **7b** suitable for X-ray crystallography were obtained from a THF (1 mL)/pentane (0.5 mL) mixture at −25 °C. $^{31}P\{^1H\}$ NMR (202.5 MHz, CD_2Cl_2, 287 K): δ_{ppm} 12.6. $^1H\{^{31}P\}$ NMR (500 MHz, CD_2Cl_2, 287 K): δ_{ppm} 7.70–7.59 (m, 2H, H_{17}), 7.40–7.36 (m, 4H, H_{16}), 7.32–7.12 (m, 4H, H_{15}), 7.23 (m, 1H, H_{13}), 7.17 (m, 2H, H_{12}), 7.12 (pseudo t, 6H, $^3J_{H,H}$ = 7.5 Hz, H_{21}), 6.87 (t, 3H, $^3J_{H,H}$ = 7.0 Hz, H_{22}), 6.77 (d, 6H, $^3J_{H,H}$ = 7.5 Hz, H_{20}), 3.30 (sept, 2H, $^3J_{H,H}$ = 6.6 Hz, -C*H*-$(CH_3)_2$), 2.40 (very br s, 3H, H_{18}), 1.80 (very br s, 3H, $H_{18'}$), 0.94 (br s, 6H, −CH(C*H*$_3)_2$), 0.79 (br s, 6H, −CH(C*H*$_3)_2$). $^{13}C\{^1H\}$ NMR (125.3 MHz, CD_2Cl_2, 287 K): δ_{ppm} 150.5 (C_{19}), 145.4 (d, $^3J_{C,P}$ = 5.5 Hz, C_{11}), 141.3 (d, $^2J_{C,P}$ = 6.9 Hz, C_{10}), 133.6 (br d, $^2J_{C,P}$ = 9.0 Hz, C_{15}), 133.3 (d, $^4J_{C,P}$ = 2.7 Hz, C_{17}), 128.9–129.1 (d, $^3J_{C,P}$ = 13.1 Hz, C_{16}), 127.9 (C_{21}), 126.4 (C_{20}), 125.4 (C_{13}), 124.9 (C_{12}), 120.9 (C_{22}), 78.5 (C_{18}), 73.5 (very br, C_1), 28.6 (*C*H$(CH_3)_2$), 23.9–24.5 (CH(C*H*$_3)_2$). Mp: 129–130 °C dec.

Synthesis of $ZrBn_3(Ph_2IndP{=}NMes)$ (7c). A solution of **4c** (200 mg, 0.46 mmol) and $ZrBn_4$ (230 mg, 0.50 mmol) in toluene (1.5 mL) was stirred at room temperature in the absence of light for 4 h. The reaction can also be performed in diethyl ether (8 mL). Although a slightly longer reaction time (14 h) was required, probably due to the poor solubility of **4c** in this solvent, the resulting complex **7c** directly precipitated from the reaction mixture, which facilitated the workup. The yellow precipitate was washed with toluene (0.5 mL), and **7c** was obtained as a yellow powder (0.26 g, 70%). Orange crystals of **7c** suitable for X-ray crystallography were obtained from a dichloromethane (0.5 mL)/pentane (1 mL) mixture at −10 °C. $^{31}P\{^1H\}$ NMR (202.5 MHz, CD_2Cl_2): δ_{ppm} 13.4. $^1H\{^{31}P\}$ NMR (500 MHz, CD_2Cl_2): δ_{ppm} 7.70 (d, 1H, $^3J_{H,H}$ = 8.0 Hz, H_6), 7.78 and 7.67 (br s, 1H each, H_{17}), 7.57 and 7.34 (br s, 2H each, H_{16}) 7.34 and 6.98 (br s, 2H each, H_{15}), 7.27 (m, 1H, H_5), 7.08 (m, 6H, H_{21}), 7.02 (m, 1H, H_4), 6.97 (dd, 1H, $^3J_{H,H}$ = 4.2 Hz, $^4J_{H,P}$ = 3.1 Hz, H_8), 6.94 (d, 1H, $^3J_{H,H}$ = 4.2 Hz, $^3J_{H,P}$ = 2.6 Hz, H_9), 6.87 (m, 5H, H_{22} and H_{12}), 6.52 (d, 6H, $^3J_{H,H}$ = 7.5 Hz, H_{20}), 6.33 (d, 1H, $^3J_{H,H}$ = 8.5 Hz, H_3), 2.32 (s, 3H, *p*-C*H*$_3$), 2.19 (br d, 3H, $^3J_{H,H}$ = 10.0 Hz, H_{18}), 1.95 (m, 9H, overlapped *o*-C*H*$_3$ and $H_{18'}$). $^{13}C\{^1H\}$ NMR (125.3 MHz, CD_2Cl_2): δ_{ppm} 148.1 (C_{19}), 141.5 (d, $^2J_{C,P}$ = 6.7 Hz, C_{10}), 137.5 (d, $^3J_{C,P}$ = 12.3 Hz, C_7), 134.9 (d, $^3J_{C,P}$ = 4.9 Hz, C_{11}), 134.5 (d, $^2J_{C,P}$ = 13.0 Hz, C_2), 134.3 (C_{13}), 134.0 and 133.5 (br s, C_{17}), 132.7 and 132.0 (br d, $^2J_{C,P} \approx$ 7.0 Hz, C_{15}), 129.0 and 128.5 (br d, $^3J_{C,P} \approx$ 10.0 Hz C_{16}), 128.2 (C_{21}), 127.0 (C_{20}), 124.3 (C_4), 124.0 (d, $^3J_{C,P}$ = 11.9 Hz, C_8), 123.4 and 123.3 (C_4 or C_5), 121.5 (C_{22}), 121.0 (d, $^2J_{C,P}$ = 11.0 Hz, C_9), 120.9 (C_4), 79.1 (C_{18}), 71.3 (d, $^1J_{C,P}$ = 118.7 Hz, C_1), 21.4 (*o*-C*H*$_3$), 20.4 (*p*-C*H*$_3$).

Synthesis of Complex 8c. A solution of **7c** (100 mg, 0.12 mmol) in toluene (2.5 mL) was heated at 80 °C in the absence of light for 5 h and evaporated to dryness. The brown residue was dissolved in dichloromethane-d_2 (0.5 mL) and transferred to an NMR tube. $^{31}P\{^1H\}$ NMR (202.5 MHz, CD_2Cl_2,): δ_{ppm} 7.4. $^1H\{^{31}P\}$ NMR (500.3 MHz, CD_2Cl_2): δ_{ppm} 7.98 (dd, 2H, $^3J_{H,H}$ = 7.2 Hz, $^3J_{H,P}$ = 12.9 Hz, H_{15}), 7.85 (t, 1H, $^3J_{H,H}$ = 7.5 Hz, H_{17}), 7.71 and 7.65 (dt, 2H, $^3J_{H,H} \approx$ 8.0 Hz, $^3J_{H,P} \approx$ 3.0 Hz, H_{16}), 7.57 (br d, 1H, $^3J_{H,H}$ = 8.5 Hz, H_6), 7.55–7.49 (m, 3H, $H_{15 \text{ and } 17}$), 7.35 (m, 1H, H_5), 7.12–7.00 (m, 4H, H_{21}), 7.03 (overlapped, 1H, H_4), 6.90–6.80 (m, 2H, H_{22}), 6.93 (d, 1H, $^3J_{H,H}$ = 3.8 Hz, H_8), 6.74 (d, 2H, $^3J_{H,H}$ = 7.5 Hz, H_{20}), 6.73 (s, 1H, H_{12}), 6.67 (d, 1H, $^3J_{H,H}$ = 8.0 Hz, H_{20}), 6.54 (d, 1H, $^3J_{H,H}$ = 7.5 Hz, H_{20}), 6.41 (s, 1H, $H_{12'}$), 6.27 (d, 1H, $^3J_{H,H}$ = 3.8 Hz, H_9), 6.11 (d, 1H, $^3J_{H,H}$ = 8.5 Hz, H_3), 2.53 (d, 1H, $^3J_{H,H}$ = 13.8 Hz, Zr-C*H*$_2$-*o*-Mes), 2.43 (d, 1H, $^3J_{H,H}$ = 13.8 Hz, Zr-C*H*$_2$-*o*-Mes), 2.27 (s, 3H, *o*-C*H*$_3$), 2.07 (d, 1H, $^3J_{H,H}$ = 9.9 Hz, H_{18}), 1.99 (d, 1H, $^3J_{H,H}$ = 9.9 Hz, $H_{18'}$), 1.60 (s, 3H, *p*-C*H*$_3$), 1.19 (d, 1H, $^3J_{H,H}$ = 9.7 Hz, H_{18}), –0.06 (d, 1H, $^3J_{H,H}$ = 9.7 Hz, $H_{18'}$). $^{13}C\{^1H\}$ NMR (125.3 MHz, CD_2Cl_2): δ_{ppm} 150.6 (C_{19}), 147.6 (d, $^2J_{C,P}$ = 19.7 Hz, C_{10}), 143.1 ($C_{19'}$), 141.5 (d, $^2J_{C,P}$ = 6.7 Hz, C_{10}), 137.5 (d, $^3J_{C,P}$ = 12.3 Hz, C_7), 134.9 (d, $^3J_{C,P}$ = 4.9 Hz, C_{11}), 134.5 (d, $^2J_{C,P}$ = 13.0 Hz, C_2), 132.9 and 133.7 (d, $^4J_{C,P}$ = 3.0 Hz, C_{17}), 131.3 and 132.8 (d, $^2J_{C,P} \sim$ 10–11 Hz, C_{15}), 129.6 and 129.7 (br d, $^3J_{C,P} \approx$ 12.6 Hz, C_{16}), 128.3 and 128.1 (C_{20}), 128.2 (C_{22}), 127.9

and 128.1 (C_{21}), 126.5 and 126.7 (br s, C_{12}), 125.9 (d, $^2J_{C,P} = 12.9$ Hz, C_2), 125.3 (C_4 or C_5), 125.1 (C_4 or C_5), 124.1 (C_6), 122.4 (C_3), 119.5 (d, $^2J_{C,P} = 14.3$ Hz, C_9), 114.6 (d, $^2J_{C,P} = 11.9$ Hz, C_8), 89.6 (d, $^3J_{C,P} = 2.8$ Hz, Zr-*C*H$_2$-Mes), 72.7 (d, $^1J_{C,P} = 127.1$ Hz, C_1), 65.7 and 62.3 (C_{18}), 22.6 (*o*-*C*H$_3$), 20.3 (*p*-*C*H$_3$).

Crystal Structure Determination of Complexes 5a and 7a–c. Data for all structures were collected at 193(2) K using a oil-coated shock-cooled crystal on a Bruker-AXS CCD 1000 diffractometer with Mo Kα radiation ($\lambda = 0.7103$ Å). Semiempirical absorption corrections were employed.[52] The structures were solved by direct methods (SHELXS-97)[53] and refined using the least-squares method on F^2.[54]

Computational Details. Zirconium and phosphorus were treated with a Stuttgart-Dresden pseudopotential in combination with their adapted basis set.[55] In all cases, the basis set has been augmented by a set of polarization functions (f for Zr and d for P).[56] Carbon, nitrogen, and hydrogen atoms have been described with a 6-31G(d,p) double-ζ basis set.[57] Calculations were carried out at the DFT level of theory using the hybrid functional B3PW91.[58] Geometry optimizations were carried out without any symmetry restrictions, and the nature of the *extrema* (*minimum*) was verified with analytical frequency calculations. All of these computations have been performed with the Gaussian 98[59] suite of programs. The electronic density has been analyzed using the natural bonding analysis (NBO) technique.[60]

Acknowledgment. We are grateful to the CNRS, UPS, and ANR program (project BILI) for financial support of this work. CalMip (CNRS, Toulouse, France) is acknowledged for calculation facilities. L.M. thanks the Institut Universitaire de France. H.G. is acknowledged for his assistance in the X-ray diffraction analysis of complex **5a**.

Note Added after ASAP Publication. In the version of this paper posted on the Web on December 5, 2007, due to a production error, the artwork for Figure 3 was incorrect and a small error was introduced into ref 46. The version of this paper that now appears is correct.

Supporting Information Available: Complete atom numbering for the NMR assignments; complete ref 59 citation; Cartesian coordinates for the optimized complexes **5a*/5c*/6c*/7a–c*/8c*** and crystallographic data for ligands **2c/4b** and complexes **5a/7a–c** (CIF). This material is available free of charge via the Internet at http://pubs.acs.org.

OM700974G

(52) SADABS, Program for data correction, Bruker-AXS, version 2.10, 2003.
(53) Sheldrick, G. M. *Acta Crystallogr.* **1990**, *A46*, 467.
(54) Sheldrick, G. M. SHELXL-97, Program for Crystal Structure Refinement, University of Göttingen, 1997.
(55) (a) Andrae, D.; Haeussermann, U.; Dolg, M.; Stoll, H.; Preuss, H. *Theor. Chim. Acta* **1990**, *77*, 123. (b) Bergner, A.; Dolg, M.; Kuechle, W.; Stoll, H.; Preuss, H. *Mol. Phys.* **1993**, *80*, 1431.
(56) Ehlers, A. W.; Böhme, M.; Dapprich, S.; Gobbi, A.; Höllwarth, A.; Jonas, V.; Köhler, K. F.; Stegmann, R.; Veldkamp, A.; Frenking, G. *Chem. Phys. Lett.* **1993**, *208*, 111.
(57) Hariharan, P. C.; Pople, J. A. *Theor. Chim. Acta* **1973**, *28*, 213.
(58) (a) Becke, A. D. *J. Chem. Phys.* **1993**, *98*, 5648. (b) Burke, K.; Perdew, J. P.; Yang, W. *Electronic Density Functional Theory: Recent Progress and New Directions*; Dobson, J. F., Vignale, G., Das, M. P., Eds.; Springer: Berlin, 1998.
(59) Frisch, M. J.; et al. *Gaussian 98, Revision A.11*, Gaussian, Inc., Pittsburgh, PA, 1998.
(60) Reed, A. E.; Curtiss, L. A.; Weinhold, F. *Chem. Rev.* **1988**, *88*, 899.